SYNTHESIS AND CHARACTERIZATION OF POLYMER-BLEND/TiO_2 NANOCOMPOSITES

BY

ABDULSALAM ISMA'ILA

(M.Sc./SCIE/013037/2007-2008)

SUBMITTED TO

DEPARTMENT OF PHYSICS

AHMADU BELLO UNIVERSITY, ZARIA, NIGERIA

IN PARTIAL FULFILLMENT OF THE AWARD OF

MASTERS OF SCIENCE DEGREE IN SOLID-STATE PHYSICS/MATERIALS SCIENCE

SUPERVISORS:

1. DR. P. O. AKUSU

2. DR. T. O. AHMED

NOVEMBER, 2012.

DECLARATION

I declare that the work in the dissertation entitled "Preparation and Characterization of Polymer-blend/TiO_2 Nanocomposites" has been performed by me in the Department of Physics, Ahmadu Bello University Zaria, under the supervision of Dr. P.O. Akusu and Dr. T.O. Ahmed.

The information derived from literature has been duly acknowledged in the text and a list of references provided. No part of this work was previously presented for another degree or diploma at any university.

_____ Date:_____

Ismaila, Abdulsalam

CETIFICATION

This dissertation entitled "Preparation and Characterization of Polymer-blend/TiO_2 Nanocomposites" by Ismaila, Abdulsalam meets the regulations governing the award of Masters of Science degree of Ahmadu Bello University, Zaria, and is approved for its contribution to knowledge and literary presentation.

_____	_____	_____
Chairman, Supervisory Committee (Dr. P.O. Akusu)	(Signature)	(Date)
_____	_____	_____
Member, Supervisory Committee (Dr. T.O. Ahmed)	(Signature)	(Date)
_____	_____	_____
Head of Department (Dr. U. Sadiq)	(Signature)	(Date)
_____	_____	_____
Dean, School of Postgraduate Studies (Prof. A. A. Joshua)	(Signature)	(Date)

DEDICATION

This work is dedicated to my parents, late Malam Ismaila Adamu (Galadiman Abakwa) and Malama Khadija Ismaila for all they have done and still doing for me. To my wife Zulaihat, my children Ismaila (Abba) and Muhammad (Sultan) for their love, endurance, encouragement and support throughout the period of my study.

ACKOWLEDGEMENT

All praises are due to Allah (S.W.T.), my creator, for His continued blessings and guidance as well as His protection.

The successful completion of this work is a result of assistance from so many people. Among them, I am especially grateful to my supervisors Dr. P.O. Akusu and Dr. T.O. Ahmed for their tireless guidance throughout the period of this research work.

I also like to thank all the lecturers of physics department for taking their time to contribute in one way or the other towards the betterment of this work.

Particular thank goes to Mr. Ifeanyi J. of NARICT Zaria, Malam M. Bashir of ABU Multi-user Science Research Laboratory, Mr. M. Bobai of NILEST Zaria, Mr. A. Noble, Mr. Kenneth A., Mrs. Unwana all of SHESTCO Abuja whose tremendous support aided a lot in the successful conduct of most of my experiments.

Finally, I am grateful to my family, parents, brothers and sisters for their love and support and to all my friends for their understanding, advice, assistance and valuable friendship. Thank you all! May the Almighty bless you all.

ABSTRACT

The polymer-blend/ TiO_2 nanocomposites are achieved via a two-stage reaction involving synthesis of TiO_2 nanoparticles and their subsequent mixing with the host polymer- blend matrix employing solution-mixing technique commonly referred to as one-pot reaction. The nanoparticles are characterized by a combination of Scanning Electron Microscopy (SEM) and Energy Dispersive X-ray Spectroscopy (EDS). The SEM-EDS analysis reveals TiO_2 to be almost isomorphic ($\geq 99\%$ phase purity) spherical in shape and particles' diameters in the range 25-40 nm. Structural modifications are studied via Fourier Transform Infra-Red (FTIR) Spectroscopy, Scanning Electron Microscopy (SEM) and X-ray Diffraction (XRD) analysis. The FTIR reveals that significant absorptions below 900 cm^{-1} represent Titanium bond organic groups and Oxygen. Other prominent functional groups occurring in the range 1076.30 cm^{-1} - 3483.56 cm^{-1} reflect the additivity of polyvinyl alcohol and polyvinyl acetate. XRD analysis shows that the materials are semi-crystalline in nature with percentage crystallinity as high as 67.6 ± 0.7%. The sizes of the crystallites are large with values in the range 1688 nm - 4589 nm. The SEM reveals that the crystallites have wider diameters with values ranging from 119 ± 5 μm to 179 ± 4 μm which is in good agreement with the sizes obtained from XRD analysis. UV-Vis Spectrophotometry shows that only sample with 1% TiO_2 absorb in the UV and Visible ranges. The samples containing 2%, 3% and 4% TiO_2 nanoparticles are transparent to UV light and show strong absorption of the visible light in the wavelength ranges of 520 nm, 590 nm and 550 nm respectively.

TABLE OF CONTENTS

Declaration - - - - - - - - - i

Certification - - - - - - - - - ii

Dedication - - - - - - - - - iii

Acknowledgement - - - - - - - - - iv

Abstract- - - - - - - - - - v

Table of contents - - - - - - - - - vi

List of Figures- - - - - - - - - - ix

List of Tables - - - - - - - - - - x

List of Abbreviations- - - - - - - - - xi

CHAPTER ONE - - - - - - - - 1

1.0 Introduction - - - - - - - - 1

1.1 Background- - - - - - - - - 1

1.2 Composite Materials- - - - - - - - 2

1.2.1 Polymer Nanocomposites - - - - - - 3

1.2.2 Inorganic Nanoparticles - - - - - - - 7

1.2.3 Justification of the Research- - - - - - - 8

1.3 Aims and Objectives - - - - - - - 9

CHAPTER TWO - - - - - - - - 10

LITERATURE REVIEW- - - - - - - - 10

2.1 Introduction- - - - - - - - 10

2.2 Review of Some Previous works-- - - - - - 11

2.3 Synthesis of Nanocomposites- - - - - - - 13

2.4 Characterization of Nanocomposites - - - - - 14

2.4.1 X-ray Diffraction- - - - - - - 14

2.4.1.1 X-rays Scattering by Crystalline Solid- - - - - 15

2.4.1.2 X-ray Diffractometer - - - - - - - 17

2.4.2 Scanning Electron Microscopy (SEM))- - - - - 19

2.4.3 Energy Dispersive X-ray Spectroscopy (EDS) - - - - 21

2.4.4 Fourier Transform Infra Red Spectroscopy (FTIR)- - - - 22

2.4.5 Transmission Electron Microscopy (TEM - - - - - 22

2.4.6 Thermal Analysis- - - - - - - - 23

2.5 Applications of Polymer Nanocomposites- - - - - 24

2.5.1 Flame Retardancy- - - - - - - - 24

2.5.2 Solar Cells - - - - - - - - 24

2.5.3 Membrane for Gas Permeability- - - - - - 24

2.5.4 Gas Barrier Performance- - - - - - - 25

CHAPTER THREE - - - - - - - - 26

MATERIALS AND METHODS- - - - - - - 26

3.0 Introduction- - - - - - - - 26

3.1 Materials - - - - - - - - - 26

3.2 Poly (vinyl alcohol) (PVA_L) - - - - - - 27

3.2.1 Properties of PVA_L - - - - - - - 27

3.2.2 Uses of PVA_L - - - - - - - - 27

3.3. Poly (vinyl acetate) PVA_C- - - - - - - 28

3.4 Titanium Dioxide ($TiO_{2)}$ - - - - - - - 28

3.5 Methodology- - - - - - - - - 28

3.5.1 Preparation of TiO_2 Nanoparticles (NPs)- - - - - 29

3.5.2 Sample Preparation - - - - - - - 29

CHAPTER FOUR - - - - - - - - 32

RESULTS AND DISCUSSION- - - - - - - 32

4.0 Introduction- - - - - - - - - 32

4.1 Scanning Electron Microscopy (SEM) and Energy Dispersive X-ray Spectroscopy (EDS) of TiO_2 Nanoparticles-- - - - - 32

4.2 Fourier Transform Infrared Spectroscopy (FTIR)- - - - 33

4.2.1 FTIR Spectra of Poly (vinyl alcohol), Poly (vinyl acetate), Polymer Blend and Functionalized TiO_2 - - - - - - 35

4.2.2 FTIR Spectra of Polymer Blend)/TiO_2 Nanocomposites- - - 35

4.3 X-Ray Diffraction Analysis of Polymer Blend/ TiO_2 Nanocomposites- - 40

4. Scanning Electron Microscopy (SEM) of the Polymer blend/TiO_2 NCs- - 45

4.5 UV-Visible Spectrophotometry - - - - - - - - 49

4.5.1 UV-Visible Spectra of Polymer Blend/TiO_2 Nanocomposites - - 50

CHAPTER FIVE - - - - - - - - 53

SUMMARY, CONCLUSION AND RECOMMENDATIONS - - 53

5.1 Summary - - - - - - - - - 53

5.2 Conclusion- - - - - - - - - 53

5.3 Recommendations- - - - - - - - - 54

REFERENCES - - - - - - - - 56

LIST OF FIGURES

Fig 2.1: Scattering of an X-ray beam by a crystal. 16

Fig 2.2: Equivalence of n = 2 for the (100) reflection and n = 1 for the (200) reflection. 17

Fig 2.3: An X-ray Diffractometer. 18

Fig 2.4 (a): XRD pattern of pure natural rubber. 18

Fig 2.4 (b): XRD pattern of Fe_2O_3 dispersed natural rubber. 19

Fig 2.5: SEM image of Fe_2O_3 dispersed natural rubber. 21

Fig 3.1: Flow chart for the general sample preparation and characterization. 31

Fig 4.1: (a) Surface morphology of TiO_2. (b) EDS spectra of TiO_2. 33

Fig 4.2: FTIR Spectra of (a) Poly (vinyl alcohol), (b) Poly (vinyl acetate), (c) Polymer Blend and (d) Functionalized TiO_2. 34

Fig 4.3: FTIR Spectra of Polymer-blend Nanocomposites containing: (a) 1% of TiO_2, (b) 2% of TiO_2, (c) 3% of TiO_2 and (d) 4% of TiO_2. 36-38

Fig 4.4 & 4.5: (a-d): X-ray Diffraction Patterns of Polymer Blend/TiO_2 Nanocomposites (Scattering Intensity versus the Scattering Angle, 2θ) 43-44

Fig 4.6 & 4.7: Scanning Electron Microscopy Images of Polymer Blend/TiO_2 Nanocomposites containing: (a) 1%, (b) 2%, (c) 3% and (d) 4% of TiO_2 47-48

Fig 4.8: UV-Vis spectra of Polymer-Blend/TiO_2 Nanocomposites containing: (a) 1%, (b) 2%, (c) 3% and (d) 4% of TiO_2 51

LIST OF TABLES

Table 4.1: Assignment of Different IR Peaks of Polymer Blend/TiO_2 Nanocomposites with the Corresponding Absorption Bands 39

Table 4.2: Peak Positions (2θ), d-spacing and Relative Intensity of Polymer Blend/TiO_2 Nanocomposites 42

Table 4.3: Calculated Values of the Average Crystallite Size D_c(nm) and Percentage Crystallinity X_c(%) 45

Table 4.4: Average Particle Diameters of Polymer Blend/TiO_2 Nanocomposites from SEM Images 49

LIST OF ABBREVIATIONS

AFM-atomic force microscopy

AN-acrylonitrile

DSC- differential scanning calorimetry

DTA-differential thermal analysis

EDS-energy dispersive spectroscopy

EVA-ethylene vinyl acetate

F.TiO_2-functionalized titanium (iv) oxide

FTIR-fourier transform infrared spectroscopy

HDPE-high density polyethylene

LDPE-low density polyethylene

LVSEM- low-voltage scanning electron microscopy

MFR-melt flow rate

MMT-Montmorillonite

NCs-nanocomposites

NPs-nanoparticles

PAN-polyacrylonitrile

PE_gMA-maleic anhydride

PE-polyethylene

PEUA-poly (ether-urethane) acrylate

PNCs-polymer nanocomposites

PP-polypropylene

PVA_C-polyvinyl acetate

PVA_L-polyvinyl alcohol

PV_N-poly (vinyl nitrate)

SAXS- small-angle x-ray scattering

SEM-scanning electron microscopy

TEM-transmission electron microscopy

TGA-thermogravimetric analysis

T_g-gas transition temperature

TiO_2- titanium (iv) oxide

UV-ultraviolet radiation

Vis-visible radiation

WAXS- wide-angle x-ray scattering

XRD- X-ray diffraction

CHAPTER ONE

INTRODUCTION

1.1 BACKGROUND

Nanotechnology, the art of creation and use of materials or devices at extremely small scales, is now recognized as one of the most promising areas for technological development in the 21st century. Advanced nanotechnology tools and techniques, along with the much improved ability to understand, manipulate, and activate single molecules and nanostructures, allow materials scientists a world of possibilities. It is expected that more important discoveries will be made with hybrid or nanocomposite materials (i.e., combining very different organic, inorganic, and biological systems in one integrated structure). The materials and processes used to separate nanoscale particles in plastics, metals, or ceramics is a big part of nanocomposite technology. One of the biggest applications of these new nanocomposites is that they can be used to make ultrafine-grained structures with dimensions in the near nanoscale range, creating greater strength from much greater surface area. In materials research, the development of polymer nanocomposites is rapidly emerging as a multidisciplinary research activity whose results could broaden the applications of polymers to the great benefit of many different industries (Williams *et al.*, 2007).

Natural polymers (from the Greek *poly* meaning “many” and *meros* meaning “parts”) are found in many forms such as horns of animals, tortoise shell, shellac (from the *lac* beetle), rosin (from pine trees), asphalt, and tar from distillation of organic materials (Katz, 1998). These materials (natural polymers) began to be chemically modified in the 1800s to produce many materials. The most famous of these were vulcanized rubber, gun cotton and celluloid. Bakelite was the first synthetic polymer produced in 1909 and the first synthetic fiber (rayon) was developed in 1911 before World War I (Onuma, 2010).

The enormous use of polymeric materials is largely attributed to their unusually excellent combination of properties, low weight and ease of processing. However, for improvement of properties such as thermal, electrical and mechanical stability, e.t.c, large numbers of additives were added to polymeric matrices to form polymer matrix composite (Masoud *et al.*, 2010). It was also reported that in the last few decades, composite materials or reinforced polymer materials have taken the place of synthetic fibers and metals because of their superior and unique properties such as ultimate tensile strength, flexural modulus, temperature resistance, decreased permeability and less shrinkage with increased heat resistance (Onuma, 2010).

Innovative composites and nanocomposites are significantly widening the range of applications of thermoplastics as well as thermosets in areas such as packaging, automotive, bio-medical devices, electronics etc. The focus is to disperse nanofillers in polymer matrix and study its effect on mechanical properties and rheological behaviour. Polymers like polyethylene, polyolefin, polyamides, polystyrene and ethylene-octene copolymers have been studied with various nanofillers like nanoclay, nanotalc, carbon nanotubes and carbon nanofibers etc. (Elodie, 2009).

Polymer composites containing ferrites are increasingly replacing conventional ceramic magnetic materials because of their mouldability and reduction in cost. They are also potential materials for microwave absorbers, sensors and other aerospace applications. These flexible magnets or rubber ferrite composites are made possible by the incorporation of magnetic powders in various elastomer matrices. This modifies the physical properties of the polymer matrix considerably (Sanchez *et al.*, 2005).

1.2 COMPOSITE MATERIAL

A composite is produced via a systematic combination of two or more materials with different physical and chemical properties and distinguishable interface (Askeland, 1985). In most composite

materials, one phase is usually continuous and called the matrix, while the other phase is called dispersed phase. On the basis of the nature of the matrices, composites can be classified into four major categories:

1. Polymer Matrix Composites
2. Metal Matrix Composites
3. Ceramic Matrix Composites
4. Carbon Matrix Composites (Ratna, 2005)

Compared to other composites, polymer matrix composites have the advantage of being processed at a much lower temperature.

The quest, by scientists, to improve properties of composite materials led to the investigation of composites with lower and lower filler size; leading to the development of microcomposites. Although, several benefits such as strength and stiffness, improved solvent or fire resistance and cost reduction were realized, these materials (microcomposites) had imparted several drawbacks as brittleness and opacity. The recent trend in composite research is nanocomposites. Nanocomposites, especially polymer nanocomposites (PNCs), give a way to overcome the limitations of their traditional counterparts (Rosoff, 2002).

1.2.1 POLYMER NANOCOMPOSITES

Polymer nanocomposites are a class of materials having properties that offer significant potentials. It was commonly defined as the combination of a polymer matrix resin and inclusions (fillers) that have at least one dimension (i.e. length, width, thickness) in the nanometer size range (Yeum et al, 2010).

Nanocomposite technology has been described as the next great frontier of material science. For example, polymer resins containing well-dispersed inorganic nanofillers (e.g. TiO_2 nanoparticles) are emerging as a new class of nanocomposites. The reason is that by employing minimal addition levels of filler (< 5 wt %) inorganic nanoparticles enhance mechanical, thermal, and dimensional and barrier performance properties significantly (Liang, 2002).

In recent years, a great interest of many leading scientist in the world is attracted by prospective high performance hybrid organo-inorganic polymer composite materials because of their multiple applications. Typically, for composites' preparation (including hybrid composites), dispersed substances (particles) like metals (Ag, Au, Cu Pt), carbon, clays, $CaC0_3$, Alumina, silica, titania ($Ti0_2$) and others could be used (Tolstov *et al.*, 2008).

The effective dispersion of nanostructured "layered" inorganic materials with high aspect ratio may improve the mechanical, thermal and barrier properties of polymers, even at very low concentration. In fact, it has been reported that; for every 1 wt % addition, a property increase in the order of 10% (or more) is realized. This loading-to-performance ratio is known as the "nano-effect" (Liang et al, 2002).

According to Vaia and Wagner (2004), development of polymer nanocomposites, as with any multicomponent material, must simultaneously balance four independent areas:

(i). Constituents selection,

(ii). Cost-effective processing,

(iii). Fabrication, and

(iv). Application.

For polymer nanocomposites, a complete understanding of these areas and their interdependencies is still in its infancy, and ultimately many perspectives will develop, dictated by the final application of the specific PNC (William *et al.*, 2005).

A major challenge in polymer science is to broaden the application window of organic polymers by retaining their features (such as lightweight, ease of fabrication, exceptional processability, durability and relatively low cost) while enhancing particular characteristics like modulus, strength, fire performance and heat resistance (Berta *et al.,* 2006). The relatively poor mechanical, thermal and electrical properties of organic polymers, as compared to metals and ceramics, pose a great obstacle in this respect. Many types of polymers such as homopolymers, co-polymers, blended polymers and modified polymers are not sufficient enough to compensate the various properties demanded. Thus the alternative approach to improve these properties is to reinforce polymers with inclusions of fiber, whisker, platelets, or particles.

In polymer nanocomposites' research, the choice of polymer is usually guided mainly by their mechanical, thermal, electrical, optical and magnetic behaviours. However, other properties such as hydrophobic/hydrophilic balance, chemical stability, bio-compatibility, opto-electronic properties and chemical functionalities (i.e. solvation, wettability, templating effect, etc.) have to be considered too (Jeon et. al., 2010). The inorganic particles (inclusions or fillers) not only provide mechanical and thermal stability, but also new functionalities that depend on the chemical nature, structure, size and crystallinity of the inorganic nanoparticles (silica, transition metals oxides, metallic phosphates, nanometals, nanoclays and metal chalcogenides). Indeed, according to a team of researchers led by Sanchez (2005), the inorganic particles can implement or improve mechanical, thermal, electronic, magnetic and redox properties, density, refractive index etc.

Systems in which the inorganic particles are the individual layers of a lamellar compound – most typically smectite clay or nanocomposites of a polymer (such as nylon) embedded among layers of silicates – exhibit dramatically altered physical properties relative to the pristine polymer. For instance, polymer-silicate nanocomposites exhibit stiffness, strength and dimensional stability in two dimensions (rather than one). Due to nanometer length scale which minimizes scattering of light, nanocomposites are usually transparent. Polymer nanocomposites represent a new alternative to conventionally filled polymers. Because of their nanometer sizes, filler dispersed nanocomposites exhibit markedly improved properties when compared to the pure polymers or their traditional composites. These include increased modulus and strength, outstanding barrier properties, improved solvent and heat resistance and decreased flammability (Fleming, 2001).

Layered silicate/polymer nanocomposites exhibit superior mechanical characteristics (e.g. 40% increase of room temperature tensile strength), heat resistance (e.g. 100% increase in the heat distortion temperature) and chemical resistance (e.g. ~10 fold decrease in O_2 and H_2O permeability) compared to the neat or traditionally filled resins. These property improvements result from only a 0.1-10 vol. % addition of the dispersed nanophase (Berta *et al.*, 2006).

Organic polymer-based inorganic nanoparticle composites have attracted increasing attention due to such properties as earlier mentioned. Generally, the resultant nanocomposites display enhanced favorable properties. This led to their being widely used in various fields such as military equipments, safety, protective garments, automotive, aerospace, electronic and optical devices. Additional properties and functions, such as high mechanical properties, flame retardation, chemical resistance, UV resistance, electrical conductivity, environmental stability, water repellency, magnetic field resistance, radar absorption etc, are continuously demanded by these application areas. Moreover, the effective properties of the composites are dependent upon the properties of constituents, the volume fraction of

components, shape and arrangement of inclusions and interfacial interaction between matrix and inclusion. With recent development in the nanoscience and nanotechnology fields, the correlation of material properties with filler size has become a focal point of significant interest (Jordan *et al.*, 2005).

The coatings of magnetic particles are of special interest because of their important applications viz. technological energy transformation, magnetic recording, magnetic fluids and magnetic refrigeration system. Polymer materials have been filled with several inorganic compounds in order to increase properties like heat resistance, mechanical strength and impact resistance and to decrease other properties like electrical conductivity, dielectric constant thereby increasing the permeability for gases like oxygen and water vapor. In recent years considerable efforts have been devoted to the development of methods for the preparation of composite particles consisting of polymer cores covered with shells of different chemical composition. In several of these powders, particles covered with magnetic materials have been used as beads for gas separation, or as pigments, catalysts, coatings, flocculent, toners, raw materials recovery, drug delivery and anticorrosion protection (Manias *et al.*, 2009).

1.2.2 INORGANIC NANOPARTICLES

Compared to conventional micron-sized particles (found in microcomposites), nanoparticles have a much higher surface-to-volume ratio. As the particle size decreases, the percentage of molecules/atoms present on the surface tremendously increased (Suryanarayana *et al.*, 1992). As a result, interparticle forces such as van der Waals and electrostatic forces, as well as magnetic attraction become stronger. Without proper chemical treatment to reduce the surface energy, it is very common for nanoparticles to form clusters or agglomerates, which are challenging to disperse individually and

uniformly in the polymer matrix, thus resulting in opaque nanocomposites similar to conventional composites (Chandra *et al.*, 2008).

1.2.3 JUSTIFICATION

A common tradition in the synthesis of polymer-based composites is the reinforcement of polymers with micron-sized fillers in order to gain strength, stiffness, improve solvent or fire resistance and to simply reduce cost. Despite these and many other benefits, several drawbacks such as brittleness and opacity are imparted by these microfillers. Nanocomposites (in which nanofillers are used) give a way to overcome the limitations of their traditional counterparts (Rosoff, 2002). Because of the significant increase in interfacial interaction between inorganic and organic phases as well as size-dependent phenomena of nanoscale particles, polymer nanocomposites are capable of dramatically improving numerous favorable properties without losing the inherent good properties of the polymer such as ductility, optical transparency etc. This is an advantage that is never achieved in traditional microcomposites. In addition, property improvements in nanocomposites are achieved at a very low loading of the nanosized inorganic particles (<5 wt %) while traditional microcomposites usually require much loading of the order of 25-40 wt % (Saujanya, 2001).

It is also pertinent to mention that among many nanocomposite precursors, Titania (TiO_2) nanopowder is increasingly been investigated due to its being non-toxic, inert, a broadband UV filter, has low cost and high refractive index and is corrosive resistant (Solomon, 1998). These, and many other improvements, make polymer/TiO_2 nanocomposites a promising new class of materials. Although, one can see the commercial benefits for widespread fields, the study of TiO_2-based nanocomposites is still in its infancy and vigorous research(s) need to be carried out to explore improved synthesis technique(s)

yielding the different nanocomposite structures and to fully understand the actual structure/property relationships.

The study and exploration of the potential properties of nanocomposites is the motivation of this research. In this research, another (or a novel) perspective approach was proposed for the preparation of polymer-blend/titania nanocomposites.

1.3 AIM AND OBJECTIVES

The aim of the research is:

- To develop polymer-blend/TiO_2 nanocomposites using solution mixing (one pot reaction) technique and characterizing it using integrated techniques (SEM-EDS, FTIR, XRD SEM and UV-Vis spectrophotometer) with the view of obtaining a material with novel properties.

The technical objectives are:

- To synthesize nanosized TiO_2 using sol-gel technique
- To examine the morphology and the elemental composition of the nanocrystalline TiO_2 in order to determine its particle size and purity using SEM-EDS characterization system.
- To functionalize the nanocrystalline TiO_2 using stearic acid in toluene solution in order to modify its surface for easy dispersion in the polymer blend matrix.
- To study the morphology and structure of the produced polymer-blend/TiO_2 nanocomposites using FTIR, XRD and SEM techniques in order to ascertain the structural modification of polymer matrices.
- To study the optical properties using UV-Vis spectrophotometer.

CHAPTER TWO

LITERATURE REVIEW

2.1 INTRODUCTION

The beginning of research on nanotechnology and nanoscience can be traced back over five decades, first described in a lecture entitled “There's Plenty of Room at the Bottom” in 1959 by Richard P. Feynman (Feynman, 1960). However, it is during the past decade that nanotechnology went through a variety of disciplines. From physics to chemistry, from chemistry to biology, from materials science to electrical engineering, scientists are creating the tools and developing the expertise to bring nanotechnology out of the research laboratories and into the market place. Nanostructured composite materials (in which organic polymer and inorganic fillers are used) represent a merger between traditional organic and inorganic materials, resulting in compositions that are truly hybrid. Nature has created many (composite) materials such as diatoms, radiolarian and bone from which scientists can learn (Porter, 2000). Organic-inorganic composites with nanoscale dimensions are of growing interest because of their unique properties, and numerous potential applications such as enhancement of conductivity, toughness, optical activity, catalytic activity, chemical selectivity etc. In these materials, inorganic and organic components are mixed or hybridized at nanometer scale leading to the formation of hybrid/nanocomposite materials (Garcia, 2004).

The key to forming such novel materials is adequate understanding and manipulation of the guest-host chemistry, occurring between the polymer and the layered compounds or the nanoparticles, in order to obtain a homogenous dispersion and a good contact between polymer and added particle surfaces (Lagashetty & Venkataramen, 2005).

2.2 REVIEW OF SOME PREVIOUS WORKS

There are many types of nanocomposites that have received significant attention in the last decade for research and development. These, among others, are; polymer/inorganic particle, polymer/polymer, metal/ceramic, and inorganic based nanocomposites. However, polymer hybrid nanocomposites have attracted great interest due to the fact that inorganic filled polymer composites often exhibit remarkable improvement in material properties even with only a low percentage of the inorganic fillers (Fleming et. al., 2001). In this context, a review is presented for related/relevant researches conducted by other researchers in the field of polymer nanocomposites.

Mohan and co-workers, (1996), studied the melt intercalation of polystyrene in layered silicates. They used three analytical techniques; wide-angle x-ray Scattering (WAXS), low-voltage scanning electron microscopy (LVSEM), and differential scanning calorimetry (DSC) to study the phenomenon of direct melt intercalation of polystyrene in an organically modified mica-type layered silicate. XRD shows that the intercalation takes place slightly above the glass transition temperature (T_g) of polystyrene and is time dependent. LVSEM images show that the intercalated hybrid resembles the pristine organosilicate in appearance, except that the intercalated hybrid show voids where polymer was present in the unannealed mixture. They also concluded, from DSC measurements, that the diminishing of the Polystyrene glass transition occurred with intercalation, leading to a complete absence of a T_g trace when the entire polymer in a sample is intercalated. Although it remains unclear, according to them, whether the glass transition of the intercalated material has been effectively lowered, raised, or eliminated.

Lee *et al.*, (2001), studied the specific interaction governing the melt intercalation of clay with poly (Styrene-co-acrylonitrile) copolymers. Different mixtures of Montmorillonite (MMT) and poly (SAN) with

various acrylonitrile (AN) contents were studied to examine the effect of specific interaction. A point of interest is that there was a limit to the increase in gallery height as such there is no tendency for the gallery height to increase with the AN group content when the AN content was greater than 30 wt %. This implied that excessive attractive interaction occurred on the clay surfaces so that polymer molecules glued the two adjacent silicate layers together; consequently, the increase in the gallery height could not be accomplished (a disadvantage).

Pegoretti *et al.*, (2007), evaluated the microstructural and mechanical characteristics of high density polyethylene-clay nanocomposites prepared via melt compounding. In this work, two HDPEs with different melt flow rates and two different organo-modified clays were used. Maleic anhydride (PE_gMA) compatibilizer was used to change the relative amount of each polyethylene grafted. The results revealed that intercalation process is more effective as the matrix melt viscosity decreases (higher melt flow rate, MFR). It was also shown that the relative stiffness of the synthesized nanocomposites increases with addition of clay but with a limited enhancement of the relative yield stress.

Manias *et al.*, (2009), used commercial grade polymers and fillers to synthesized polyethylene nanocomposites heat-sealants with a versatile peelables character. The work has shown that a novel heat-sealing performance is achieved by polyethylene (PE) nanocomposites reinforced by ethylene vinyl acetate (EVA) and Montmorillonite (MMT). The materials were found to exhibit a very versatile heat-sealing behavior, yielding hermetic but peelable heat-seals across the broadest possible temperature range.

Tolstov *et al.*, (2008), in their novel work titled synthesis and Characterization of hybrid cured poly (ether-urethane) acrylate (PEUA)/titania microcomposites via swelling technique used IR, SAXS,

SEM techniques as well as gravimetric analysis to characterize the composites prepared. The gravimetric analysis showed that TiO_2 content in most of the polymer composites prepared were in the range 3.8-30.8 wt %. SAXS studies revealed nano-sized (3.5-5nm) heterogeneity of the polymer/TiO_2 composites prepared. Also using IR studies, the formation of the hybrid microcomposites via chemical interactions of high reactive carboxylic groups of poly (ether-urethane) acrylate (PEUA) constituent and tetraisopropoxititanate (TIPT) precursor was clearly confirmed. They further suggested that the data obtained in the work could be used for elaboration of high-loaded transparent or semitransparent TiO_2-filled hybrid polymer composites for multipurpose optical uses or advanced sealants.

2.3 SYNTHESIS OF NANOCOMPOSITES

The synthesis of polymer nanocomposites is an integral aspect of polymer nanotechnology. The vigorous development of polymer science and extensive utilization of polymeric materials in technology have led, in recent years, to the increased interest in the preparation and characterization of polymer and its composite films.

For traditional composite materials, high performance requires, in a first approach, homogeneous and thermodynamically stable dispersion of the fillers in the polymer matrix. To this end, the two major hurdles to be overcome are; (1) deaggregation of the filler assemblies (clusters of fillers often containing tens, hundreds, or even millions of filler particles, associated with very strong interparticle forces, and (2) achieving sufficiently strong polymer–filler interfaces, required for good mechanical coupling between the matrix and the filler. Both these requirements are also necessary in polymer-based nanocomposites (Manias *et al.*, 2007). Many methods have been reported for the preparation of polymer-based inorganic nanoparticles composites. Prominent among them are; (i) intercalation of nanoparticles with the polymer or pre-polymer from solution (Alexandre & Dubois,

2000), (ii) in-situ intercalative polymerization (Okamoto *et al.*, 2000), (iii) melt intercalation (Vaia *et al.*, 1997), (iv) direct mixture of polymer and particulates (Du et al., 2002), (v) template synthesis (Carrado & Xu, 1998), (vi) in situ polymerization (Evora & Shukla, 2003) and (vii) sol-gel process (Avadhani & Chujo, 1997).

According to Jeon & Baek (2010), polymer based nanocomposite synthesis is largely influenced by molecular weight, inorganic particles' size/content as well as properties.

2.4 CHARACTERIZATION OF NANOCOMPOSITES

Characterization is an essential part of all investigations dealing with materials. The important aspects of characterization are chemical composition and compositional homogeneity (chemical homogeneity), structure (including crystal system where possible atomic coordinates, bonding and ultra structure) and identification and analysis of defects and impurities influencing the properties of the materials. Characterization, therefore, describes all those features of composition and structure of a material that would suffice for reproducing the material. The advances made in the last few years in characterization techniques, especially in the structure elucidation, have been impressively large and have opened new vistas in solid state materials (Masoud & Dawood, 2009).

Among the several characterization techniques, X-ray diffraction (XRD), scanning electron micrography (SEM), energy dispersive X-ray spectroscopy (EDXS) and fourier transform infrared spectroscopy (FTIR) are the three important techniques. Others like atomic force microscopy (AFM), transmission electron microscopy (TEM), and differential thermal analysis (DTA) are also employed for further characterization purposes.

2.4.1 X-RAY DIFFRACTION

Von Laue (1912) discovered that crystals can act as three dimensional diffraction grating. To explore crystal structure we use diffraction patterns of waves that interact with atoms that have a wavelength comparable with interatomic spacing.

At optical wavelengths, such as 500Å, the superposition of the waves scattered elastically by the individual atoms of the crystal results in ordinary optical refraction. But when the wavelength of the radiation is comparable with or smaller than the lattice constant, we may find diffraction beams in directions quite different from the incident directions. The Laue experiments show that diffraction patterns consist of series of spots and this pattern shows the symmetry of the crystal.

The nature of bonding and the working criteria for distinguishing between short-range and long-range order of crystalline arrangements from the amorphous substances are largely derived from X-ray diffraction and thus it remains a useful tool to obtain structural information. X-ray diffraction enables the determination of the d-spacing of the filler in question. An immiscible system is obtained if the d-spacing in the presence of the polymer is unchanged from that of the pristine filler. If the d-spacing increases, it is an indication that intercalation has occurred (Bras *et al.*, 2005).

2.4.1.1 X-RAYS SCATTERING BY CRYSTALLINE SOLIDS

Scattering of X-rays from crystalline solids can be demonstrated by consideration of the diffraction from points on a set of lattice planes. Considering fig 2.1 below, the scattering of the impinging X-ray beam from points P and S in neighbouring planes will produce, in phase, diffracted X-ray beams (constructive interference) if the additional distance travelled by the X-ray photon scattered from Q is an integral number of wavelengths. This path difference SQ + QT will depend on the lattice spacing or d_{hkl},

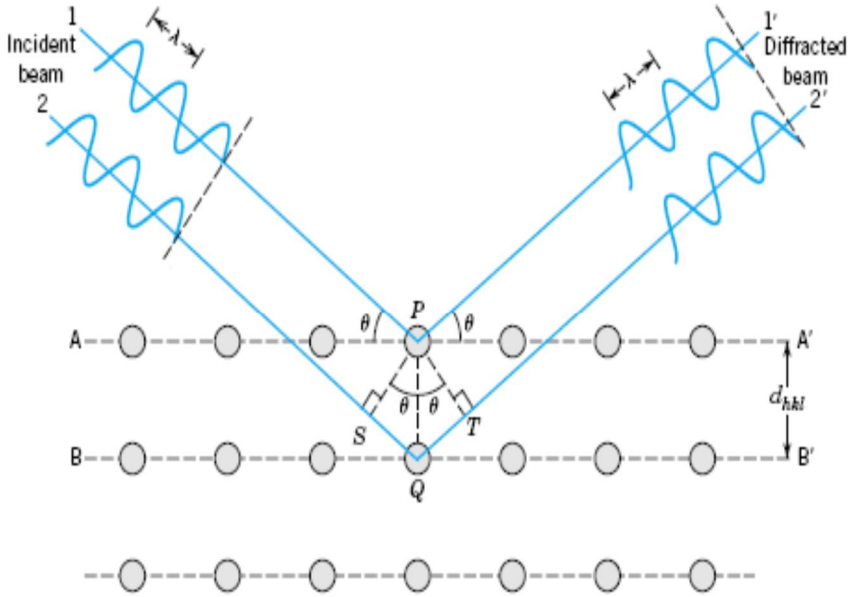


Fig 2.1: Scattering of an X-ray beam by a crystal (Callister, 1997).

where hkl are the Miller indices for the planes under consideration, and will also be related to the angle of incidence of the X-ray beam, θ. For an integral wavelength, the following relationship between θ and d_{hkl} can be obtained as

$$\text{Path difference} = SQ + QT = 2.d_{hkl}.\sin\theta = n\lambda \qquad (2.1)$$

where *n* is an integer λ is the X-ray wavelength. Expression (2.1) is known as the Bragg equation. In general n is always taken as unity; the reason for this is illustrated in the figure 2.2.

Rewriting the Bragg equation as

$$\lambda = 2(d_{hkl}/n).\sin\theta \qquad (2.2)$$

and consideration of figure 2.1 shows that the higher order diffraction, *n* = 2, is equivalent in representation to diffraction from a set of planes with half the separation. Hence, the second order diffraction from, for example, the (100) plane is identical to the first order diffraction from the (200) plane. Generally, it is always possible to select lattice planes such that *n* is unity (Weller, 1994).

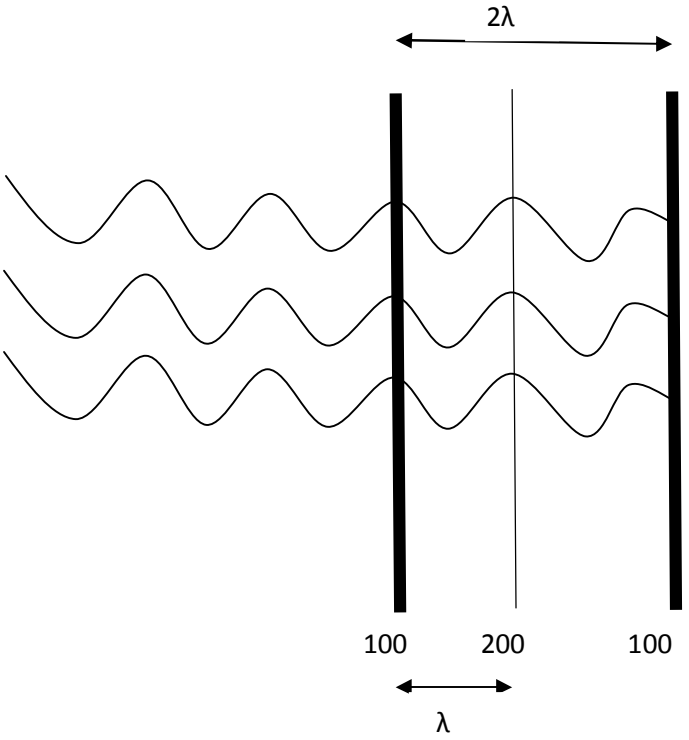


Fig. 2.2: Equivalence of n = 2 for the (100) reflection and n = 1 for the (200) reflection (Weller, 1994).

2.4.1.2 X-RAY DIFFRACTOMETER

An X-ray diffractometer is an instrument for studying crystalline and noncrystalline (amorphous) materials by measurement of the way they diffract (scatter) X-rays of known wavelength. In this instrument, the intensity of a diffracted beam is measured directly by an electronic X-ray detector. The detector converts the incoming X-rays into pulses of electric current, which are fed into various electronic components for processing. The electronics count the number of pulses per unit time and this number is proportional to the intensity of the X-ray beam entering the detector (Poole *et al.*, 2003).



Fig 2.3: An X-ray Diffractometer (Excerpt: Bruker's X-ray Diffraction D8-Discovery Instrument).

X-ray diffraction pattern of most polymers, especially amorphous polymers, will not show any sharp and highly intensed peaks whereas the nanocomposites of amorphous polymer show sharp and highly intensed peaks. This is due to the development of crystallinity in the amorphous polymer. Figures 2.4 (a) and (b) show the XRD pattern of pure natural rubber and Fe_2O_3 dispersed natural rubber composite. Highly intensed peaks occur in the pattern due to the presence of inserted iron oxide materials in the rubber matrix (Lagashetty & Venkataramen, 2005).

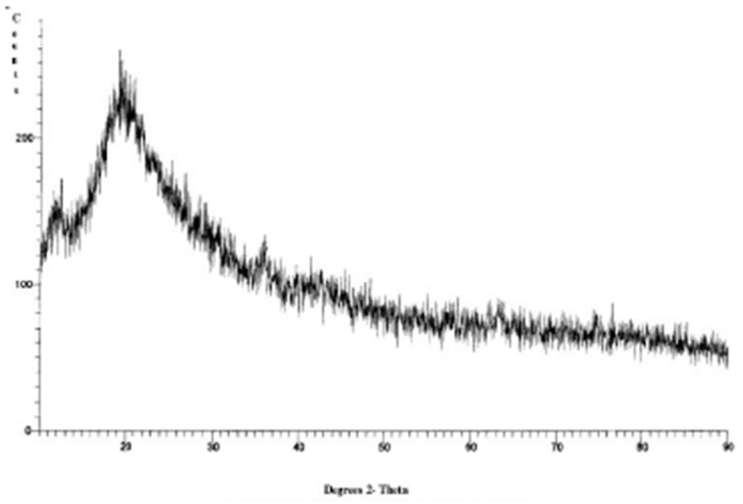


Fig.2.4 (a): XRD pattern of pure natural rubber.

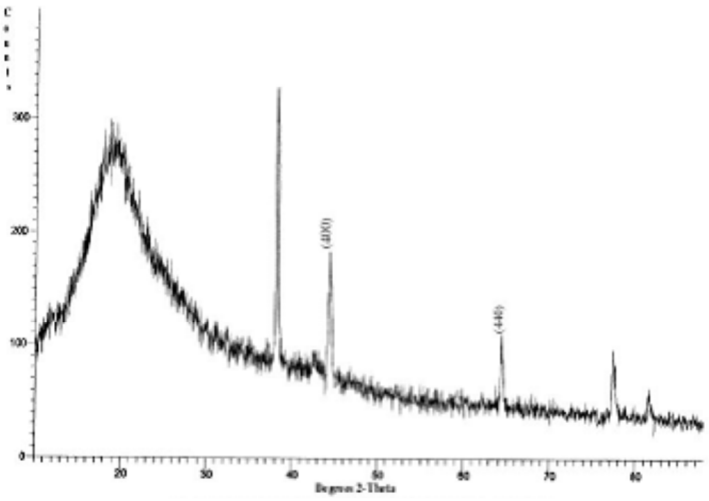


Fig.2.4 (b): XRD pattern of Fe_2O_3 dispersed natural rubber.

However, since it is found in some systems (like polymer-clay exfoliated system) that registry between the filler layers is lost, then no peak appearance is expected. Unfortunately, the same situation will occur if the filler exhibit extensive disorder. Hence XRD information alone is not enough to identify

the morphology of composites. For these reasons, in general, XRD analysis is not used alone in deducing nanocomposite morphology (Bras *et al.*, 2005).

2.4.2 SCANNING ELECTRON MICROSCOPY

Structural phenomena play an important role in determining the properties of a polymer. Mechanical properties are determined not only by the changes in shape confirmation and by motion of individual molecules of the polymers, but by the behaviour of larger and more complex structural formations as well. The interface boundaries of these formations, known as super molecular structures, are the sites where chemical reactions in the polymer are most likely to begin and centers of crack formation and incipient destruction are likely to arise. It has been found that extensive occurrences of ordered structures are typical not only of crystalline, but also of amorphous polymers (Jordan *et al.*, 2005). The shapes of most polymer molecules may vary within wide limits when studying the simplest phenomenon of structure formation.

Scanning electron microscopy determines morphology and shape of surfaces of materials. In polymer matrix nanocomposites, especially when low amount of nanoparticles is added to polymer, polymeric chains cover the nanoparticles thereby posing huge obstacle in obtaining surface images via SEM. However, when high percentage of nanoparticles is added to polymer, the nanoparticles are usually seen in the matrix (Salavati-Niasari *et al.*, 2009).

When non-conducting materials are used in SEM analysis, electric charges accumulate on the sample surface during examination and therefore obscure the fine details of the specimen that is being studied. This is not encountered in conducting materials. To avoid this, a thin film coater unit is used to form a thin film of gold layer on all samples before being analyzed. The gold film provides a good

conducting path to earth. The thickness of the film is the order of 10-100nm. The thickness of gold must, however, not be such that can obscure the fine details of the specimen being studied.

The phenomenon of structural transformations occurring during deformation is very typical of polymers. A classic example of structural transformation is the formation of a 'neck' on deformation as observed in the case of crystalline polymers (Askeland, 1985). It is also observed in the case of amorphous polymers with developed structures and it is firmly described as a phase transformation. The nature of this phenomenon remained obscure for a long time, but electron microscopy revealed that 'neck' formation is actually a jump-wise transition from one super molecular structure to another with a sharp interfacial boundary which is also observed on a microscopic scale. A well-known example is that of poly (methyl methacrylate) where a sharp boundary can be seen between the isotropic and the oriented parts of the specimen (Chandra *et al.*, 2008). Figure 2.5 shows the SEM images of Fe_2O_3 dispersed natural rubber composite. From the figure one can observe the fine dispersion of iron oxide particles in the rubber matrix. The dispersed particles have irregular shape and show agglomeration (Lagashetty & Venkataramen, 2005).

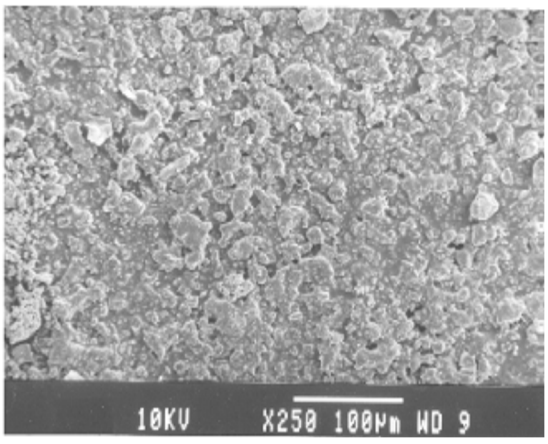


Fig. 2.5: SEM image of Fe_2O_3 dispersed natural rubber.

2.4.3 ENERGY DISPERSIVE X-RAY SPECTROSCOPY

EDS makes use of the X-ray spectrum emitted by a solid sample bombarded with a focused beam of electrons to obtain a localized chemical analysis. All elements from atomic number 4 (Be) to 92 (U) can be detected in principle, though not all instruments are equipped for 'light' elements ($Z < 10$). Qualitative analysis involves the identification of the lines in the spectrum and is fairly straightforward owing to the simplicity of X-ray spectra. Quantitative analysis (determination of the concentrations of the elements present) entails measuring line intensities for each element in the sample and for the same elements in calibration Standards of known composition.

By scanning the beam in a television-like raster and displaying the intensity of a selected X-ray line, element distribution images or 'maps' can be produced. Also, images produced by electrons collected from the sample reveal surface topography or mean atomic number differences according to the mode selected. The scanning electron microscope (SEM), which is closely related to the electron probe, is designed primarily for producing electron images but can also be used for element mapping and even point analysis if an X-ray spectrometer is added. There is thus a considerable overlap in the functions of these instruments (Russ, 1984).

2.4.4 FOURIER TRANSFORM INFRARED SPECTROSCOPY

Fourier Transform Infrared Spectroscopy (FTIR) is one of the most powerful analytical techniques, which offers the possibility of chemical identification. This technique, when coupled with intensity measurements, may be used for quantitative analysis. One of the important advantages of infrared spectroscopy over the other usual methods of structural analysis (X-ray diffraction, electron spin resonance, etc.) is that it provides information about the structure of a molecule quickly, without tiresome evaluation methods. This method can solve many problems in Solid State Physics/Chemistry

and also advantageously complements the results obtained by other methods (Jeon *et al.*, 2010). This technique is based upon the simple fact that a chemical substance shows marked selective absorption in the infrared region giving rise to close-packed absorption bands called an IR absorption spectrum, over a wide wavelength range (Lagashetty & Venkataramen, 2005). Various bands will be present in the IR spectrum, which will correspond to the characteristic functional groups and bonds present in a chemical substance. Thus an IR spectrum of a chemical substance is a fingerprint for its identification. IR spectrum of polymer nanocomposite shows the presence of both nanomaterials and polymers (depending upon the polymer chain) at various frequencies.

2.4.5 TRANSMISSION ELECTRON MICROSCOPY

Transmission electron microscopy (TEM) is employed, in its simplest bright-field mode, as a tool for direct visualization of the nanocomposite structure of polymer nanocomposites. This is possible because there exists sufficient contrast for the transmitted electrons between the polymer matrix and most filler (inorganic material such as metal oxides). In the extreme case, high-resolution TEM can even provide a qualitative picture of the inorganic filler crystal structure (Morgan & Wilkie, 2007). It is worthy of note that to obtain one TEM requires only a minuscule piece of material and one cannot be certain that this is a representative of the whole. The morphology can only be clearly determined by sampling enough of the material (Bras et al., 2005).

2.4.6 THERMAL ANALYSIS

Thermal analysis may be defined as the measurement of physical and chemical properties of materials as a function of temperature. The two main thermal analysis techniques are thermogravimetric analysis (TGA) which automatically records the change in weight of a sample as a function of either temperature or time, and the differential thermal analysis (DTA), which measures the difference in temperature, ΔT, between a sample and an inert reference material as a function of temperature; DTA therefore detects change in heat content. A technique closely related but modified to DTA is differential scanning calorimetry (DSC). In DSC, the equipment is designed to allow a quantitative measure of the enthalpy changes, (ΔH), which occurs in a sample as a function of either temperature or time**.** DSC is an analytical tool which helps to understand the thermal behavior of polymer nanocomposites. It helps in finding glass transition temperature (T_g) of polymer and its polymer composites. The increase in T_g values show the presence of inorganic materials in the polymer matrix. Exciting developments can be expected in the area of polymer nanocomposites and structures in the near future. Investigations on polymer nanocomposite can thus pay rich dividends.

2.5 APPLICATIONS OF POLYMER NANOCOMPOSITES

2.5.1 FLAME RETARDANCY

Coupled with the numerous advantages that synthetic polymeric materials provide in everyday life, there is one obvious disadvantage related to the high flammability of many synthetic polymers. Improving the fire retardant behavior of polymers is a major challenge for extending their use to most applications. Nanocomposites are very attractive in this respect, in that; small amount of nanostructure can lead to great improvement in fire resistant property of nanocomposites (Masoud & Dawood, 2010).

2.5.2 SOLAR CELLS

Polymer-based solar cells can be used to make cheap, large and flexible solar panels. Chalcogenides of cadmium; such as Cadmium Sulfide (CdS) nanoparticles in polymers, have been used in fabricating solar cells with numerous efforts to improve their efficiencies (Kothurkar, 2004). It is further reported that in addition to the high density of the nanoparticles, the control of the band edge of the particles is also a very important factor in controlling the efficiency of the solar cells.

Polymer-semiconductor nanocomposites offer a promise of a new generation of hybrid materials with numerous possibilities of applications such as in optical displays, photovoltaics, gas sensors, electrical devices, photoconductors and superconductor devices (Kothurkar, 2004).

2.5.3 MEMBRANE FOR GAS PERMEABILITY

Many inorganic types of filler have been dispersed in polymer matrix to improve pure polymeric membrane properties and constituted mixed-matrix membranes (MMMs). With addition of low amount of nanoparticles to polymeric membrane, a great increase in permeability of membrane is achieved. In fact there are many reports of improved permeability (Kim & Marand, 2008).

2.5.4 GAS BARRIER PERFORMANCE

Polymeric composites have been excellently applied in majority of research firms and industries for effective gas barrier performance. Synthetically, by addition of minute amount of alumina silicate layers to polymer matrix, gas barrier performance for nanocomposites can be obtained (Masoud & Dawood, 2010).

CHAPTER THREE

MATERIALS AND METHOD

3.0 INTRODUCTION

A brief description of the major materials used in this research as well as the experimental procedures and techniques employed are briefly described in this chapter. A descriptive approach to the preparation and characterization of TiO_2 nanoparticles using SEM-EDS system is presented. Chemical and functional groups identification via Fourier transform infrared spectroscopy (FTIR) is also described. Description of samples preparation for nanocomposites and characterization via x-ray diffraction (XRD) and scanning electron microscopy (SEM) as well as optical properties using UV-Visible spectrophotometry is presented.

3.1 MATERIALS

Starting materials used for the polymer-blend/TiO_2 synthesis include amongst others; polyvinyl alcohol; {PVA_l: $(C_2H_4O)_x$ "hydrolyzed", East Anglia Chemicals, England. No. 13970}, polyvinyl acetate; {PVA_c: $C_4H_6O_2$, BDH Limited Poole, England), and titanium chloride {$TiCl_4$, BDH Limited Poole, England} as major materials. Others include inorganic and organic reagents:

* Stearic acid {$CH_3(CH_2)_{16}\ CO_2H$; 99% purity, 67-69^{0}C M.P. & 183-184^{0}C B.P., BDH Limited Poole, England}.

* Ammonia solution {NH_3, assay; 33%, Griffin & George, England}.

* Toluene {$C_6H_5CH_3$, 99.7%, BDH Limited Poole, England}.

* Acetone {$CH_2(CH_2)_2O$, BDH Limited Poole, England}.

* Filter paper {12.5cm Grade, Whatman, England}.

* Crucible dishes, Petri dishes, Pestle, Spatulas, Mask, Hand gloves, Beakers, Measuring Cylinder, and Measuring Flask {Steve Moore Chemicals, Zaria, Nigeria}.

3.2 POLY (VINYL ALCOHOL) (PVA_l)

Polyvinyl alcohol was first prepared in 1924 by hydrolyzing polyvinyl acetate in ethanol with potassium hydroxide. However, for commercial purposes, it is prepared from acetate usually by continuous process. The acetate groups are hydrolyzed by ester exchange with methanol in the presence of anhydrous sodium methylate or aqueous sodium hydroxide (Saxena, 2004). Its physical characteristics and specific functional uses depend on the degree of polymerization and the degree of hydrolysis. As such, it is classified into two classes, namely; partially hydrolyzed and fully hydrolyzed.

3.2.1 PROPERTIES OF PVA_l

Polyvinyl alcohol, $(C_2H_4O)_x$, is an odorless, tasteless, nontoxic, translucent, and hygroscopic white or cream colored granular powder (a synthetic polymer). It has a molecular weight of between 26,300 and 30,000; density of 1.19-1.31g/cm^3 and a degree of hydrolysis of 86.5-89%. It is soluble in water, slightly soluble in ethanol and insoluble in other organic solvents. Typically, a 5% solution of polyvinyl alcohol exhibits a pH in the range of 5.0-6.5 (Saxena, 2004). PVA_l has a melting point 230^oC and 180-190^oC for the fully and partially hydrolyzed grades respectively. It decomposes rapidly above 200^oC as it can undergo pyrolysis at high temperatures. It exhibits crystallinity as the hydroxyl groups fit into the lattice without disrupting it. It also has high tensile strength and flexibility as well as high oxygen and aroma barrier properties depending on humidity (Taniguchi, 1977).

3.2.2 USES OF PVA_I

Polyvinyl alcohol is the raw material for the preparation of other polymers like polyvinyl nitrate (PVN) and polyvinyl acetals. Other commercial and industrial uses of PVA_I include: as textile sizing agent, in eye drops and hard contact lens as a lubricant, as fiber reinforcement in concrete, as surfactant for the formation of polymer encapsulated nanobeads, in protective chemical-resistant gloves, and can be used to polarize light when doped with iodine (Wikipedia search). According to Yeum *et al.*, PVA_I is a semicrystalline hydrophilic polymer with good chemical and thermal stability. It has high water permeability and can be processed easily. These properties, among others, have led to its use in wide range of applications.

3.3 POLY (VINYL ACETATE) (PVA_C)

Apart from being non-hygroscopic and less heavy, due to smaller molecular weight, PVA_C has virtually same properties and uses with its alcohol counterpart.

3.4 TITANIUM DIOXIDE (TiO_2)

Since its commercial production in the early twentieth century, titanium dioxide (TiO_2) has been widely used for a variety of applications. In 1972, Fujishima and Honda discovered the phenomenon of photocatalytic splitting of water on a TiO_2 electrode under ultraviolet (UV) light. Henceforth, enormous efforts have been devoted to the research of TiO_2 material, which has led to many promising applications in areas ranging from photovoltaics and photocatalysis to photo-electrochromics and sensors. Titanium dioxide is produced by either the sulfate or the chloride process.

Processing conditions determine the form (anatase or rutile structure) of the final product (Chen & Mao, 2007).

3.5 METHODOLOGY

As earlier mentioned, the method employed is the solution mixing technique (one-pot reaction method). It involves the direct mixing of the different components with relevant organic solvent and adequate monitoring of the reaction conditions and product(s). All the chemicals used are analytical grade.

3.5.1 PREPARATION OF TiO_2 NANOPARTICLES (NPs)

In this respect, titanium (iv) oxide nanoparticles were prepared using the acid hydrolysis technique with ammonia solution as pH adjuster.

For the preparation of TiO_2 nanoparticles, a solution of 1.5M ammonium sulfate which consisted of 0.75M titanium (IV) chloride was used. The total volume of 50ml in aqueous solution was heated at 75^{o}C and monitored at the same temperature for 90 minutes. Subsequently, ammonium hydroxide solution (2.5M) was added drop-wise under high speed stirring until the pH reached 7.0. The precipitated titanium hydroxide was collected, repeatedly washed with distilled water and ethanol and dried at 50-55^{o}C. After being calcined at 400^{o}C for 4 hours, the sample was slowly cooled at room temperature.

Titanium dioxide, as prepared, cannot be used for the mixture without some chemical modification (functionalization). This functionalization is aimed at modifying the surface of the TiO_2 in order to ensure good dispersion and bonding with the molecules of the polymer blend in which it will be introduced. The modified (functionalized) TiO_2 has the form below;

TiO_2 + Organic acid (stearic acid) = ($F.TiO_2$) 3.1

3.5.2 SAMPLE PREPARATION

Weight percentages ranging from 1-4% of $F.TiO_2$ were added separately to PVA_C and the blend of PVA_I and PVA_C using Toluene (an organic solvent). Since PVA_I is soluble in water (hydrophilic), it was dissolved in hot water (boiled at 120^oC) together with unfunctionalized TiO_2. Four samples of polymer-blend/TiO_2 were produced. The resulting samples were oven dried at temperature range of 80-100^oC for 4 hours and subsequently hot pressed using hydraulic press at temperatures close to the melting points of the polymers and the polymer-blend in order to obtain uniform polymer films.

The mixing ratios are as follows;

- $[(\text{Polyvinyl alcohol})_{\mathbf{1-z}}\ (\text{Polyvinyl acetate})_{\mathbf{z}}]_{\mathbf{1-p}} . [(F\text{-}TiO_2)_{\mathbf{p}}$

  z = 50%.

  p = 1%, 2%, 3%, and 4%.

The procedure for sample preparation/characterization can be summarized using the flow chart below;

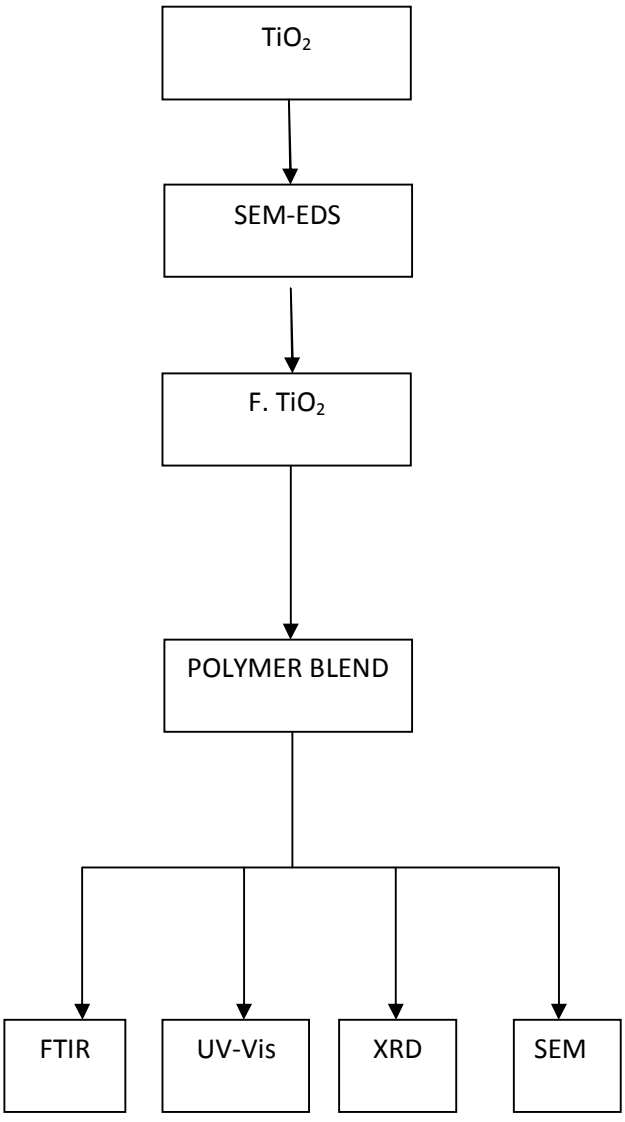


Fig 3.1: Flow chart for the general sample preparation and characterization.

CHAPTER FOUR

RESULTS AND DISCUSSION

4.0 INTRODUCTION

This chapter summarizes the analysis of the results obtained from the samples prepared for this study. These include characterization of the TiO_2 nanofiller using Scanning Electron Microscopy (SEM) and Energy-Dispersive X-ray Spectroscopy (EDS) as well as the characterization of the polymer blend/TiO_2 nanocomposites using Fourier Transform Infrared Spectroscopy (FTIR), UV-visible Spectroscopy, X-ray Diffraction (XRD) and Scanning Electron Microscopy (SEM)

4.1 Scanning Electron Microscopy (SEM) and Energy Dispersive X-ray Spectroscopy (EDS) of TiO_2 Nanoparticles

Surface morphology of the synthesized TiO_2 nanoparticles was observed using EVOI MA10 (ZEISS) multipurpose scanning electron microscope operating at 20 kV employing secondary electron signals.

The image presented in figure 4.1 together with the corresponding EDS spectra obtained using characteristic x-rays emitted by TiO_2 nanoparticles was observed at a magnification of 67.45 kX. The uniform contrast in the image revealed TiO_2 to be almost isomorphic. Nevertheless, Oxygen and Nitrogen occur with minor concentrations as impurities thereby making Ti the dominant element with concentration of about 99.5% as depicted in the EDS spectra (fig 4.1b).

The morphology of TiO_2 nanoparticles is such that the particles are closely parked and spherical in shape. The average diameter of the particles is in the range of 25-40 nm reflecting that TiO_2 nanoparticles are transparent and suitable filler for polymer composite applications.

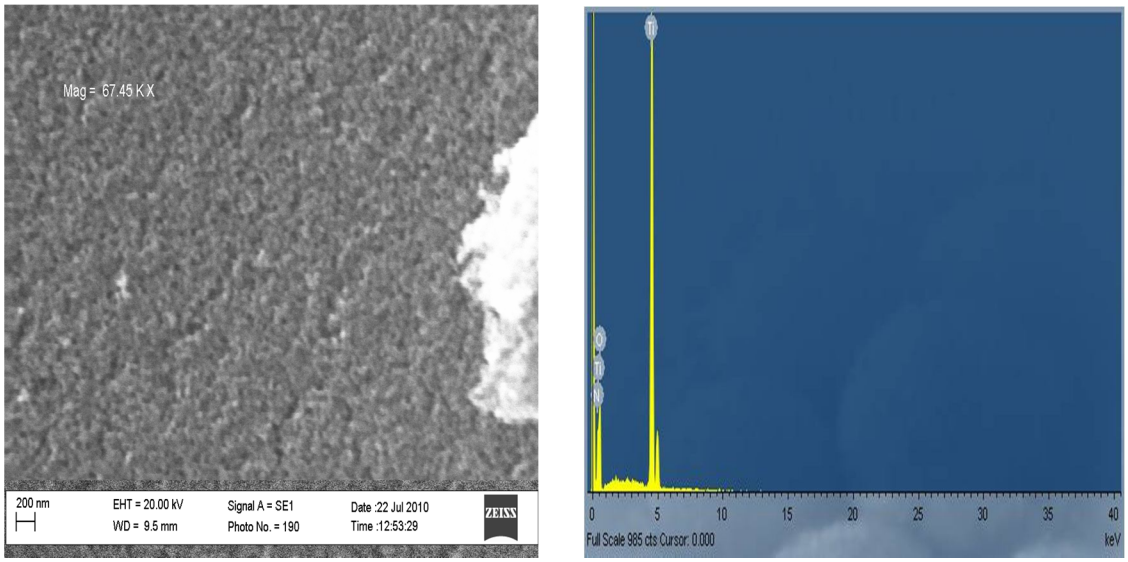
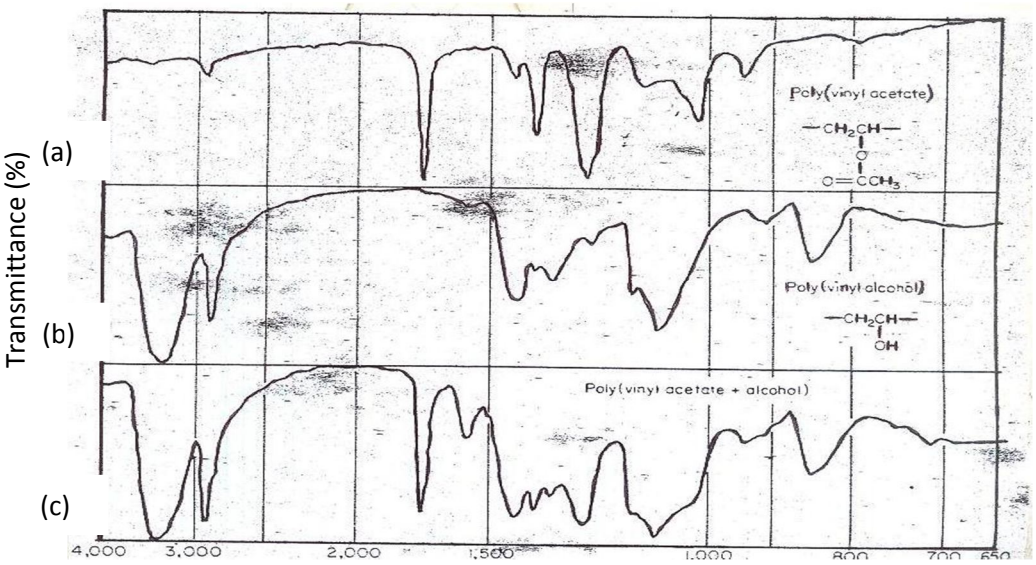


Fig 4.1: (a) Surface morphology of TiO_2. (b) EDS spectra of TiO_2.

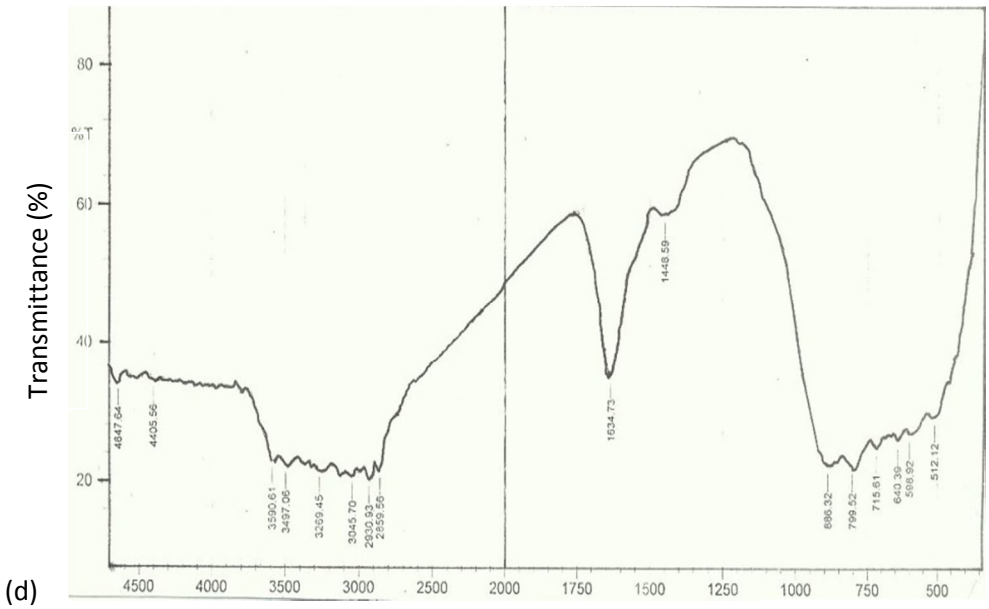
4.2: **Fourier Transform Infrared Spectroscopy (FTIR)**

As captured earlier, the FTIR analysis is employed in order to identify if the TiO_2 nanoparticles were embedded in the matrices and chemically bonded to polymer chains. The FTIR spectra of all the component reagents, polymer blend and the prepared nanocomposite samples were obtained using SHIMADZU FTIR-8400S spectrophotometer at National Research Institute for Chemical Technology (NARICT) Zaria.

It is an established fact that the fundamental vibrations of solids (fingerprints) are localized in the low frequency region (<1200 cm^{-1}) of the midrange (400-4000 cm^{-1}) of the infrared (IR) spectrum. Also, as reported by Morterra *et al.*, (1996) the Ti-O bond is clearly located in the range from 400-900 cm^{-1}. In this work, the significant absorptions observed below 900cm^{-1} represent Ti bonds with vinyl groups, secondary alcohols, carbonyl groups and oxygen.



Wave number (cm^{-1})



Wave number (cm^{-1})

Fig 4.2: FTIR Spectra of (a) Poly (vinyl alcohol), (b) Poly (vinyl acetate), (c) Polymer Blend and (d) Functionalized TiO_2.

4.2.1: **FTIR Spectra of Poly (vinyl alcohol), Poly (vinyl acetate), Polymer Blend and Functionalized TiO_2 Nanoparticles**

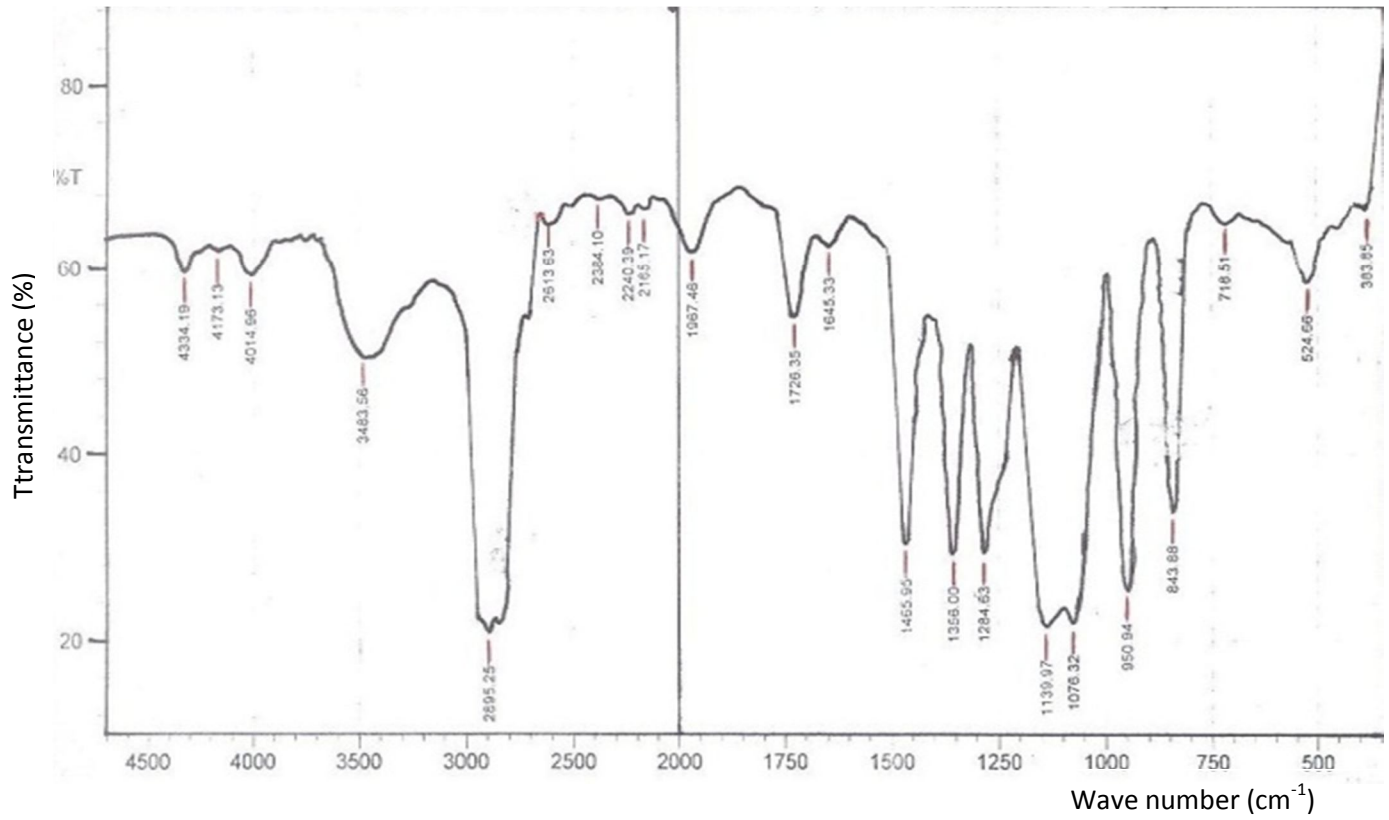
The spectra for the functionalized TiO_2 nanoparticles, poly (vinyl alcohol), poly (vinyl acetate), polymer blend (poly (vinyl acetate + vinyl alcohol)) and the functionalized TiO_2 are given in fig. 4.2 (a-d). The prominent functional groups in poly (vinyl alcohol), poly (vinyl acetate) and the blend are OH stretching vibrations, CH_2 stretching and bending vibrations, CH_3 bending vibrations, C-O-C vibration in esters, vC=O stretching vibration, C-OH stretching vibrations, CH bending and C=O stretching vibration. They are basically the hydroxyl groups, vinyl groups, acetates, alcohols and carbonyl groups.

The functional groups in the modified TiO_2 nanoparticles are also presented in table 4.1. These comprise of hydroxyl group, organic group, carbonyl group and the functional groups of the modified TiO_2 surface.

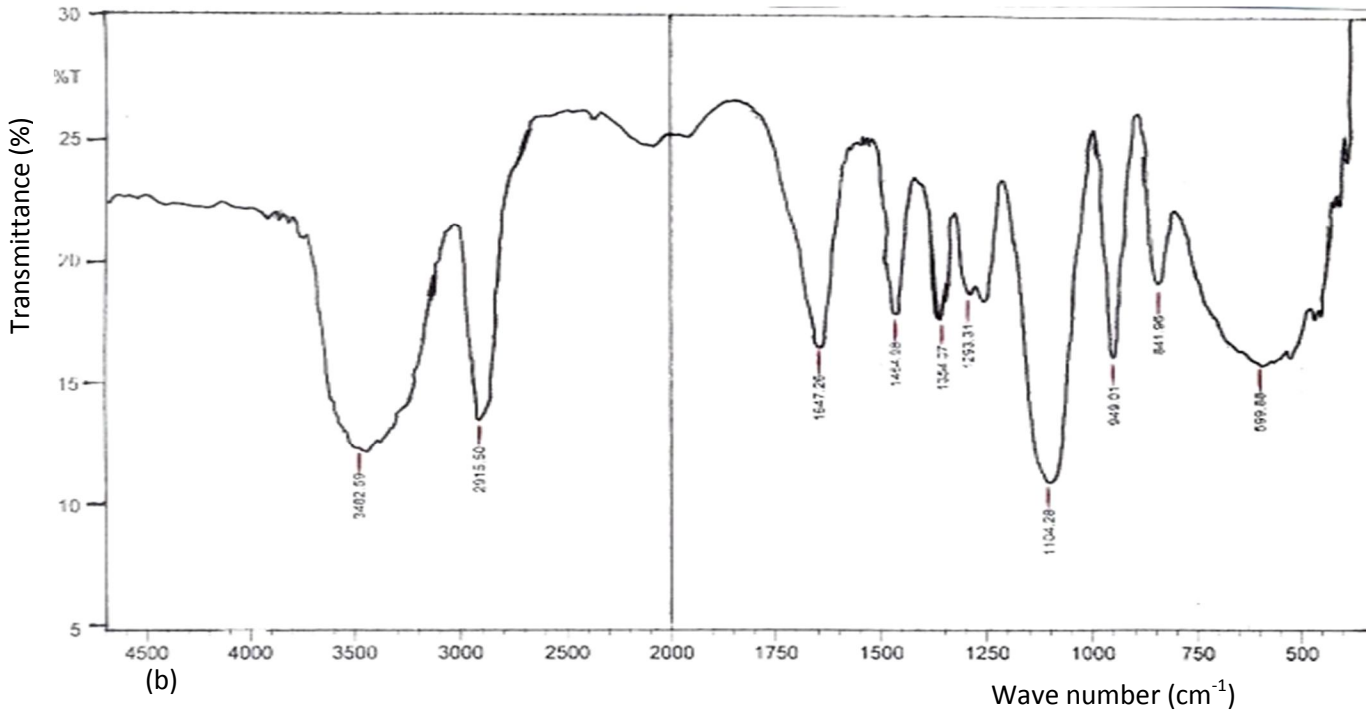
4.2.2: **FTIR Spectra of Polymer-Blend/TiO_2 Nanocomposites**

The observed spectra of the polymer-blend/TiO_2 nanocomposites reveal the additivity of the spectra of poly (vinyl alcohol)/ TiO_2 and poly (vinyl acetate)/ TiO_2. In figs 4.3 (a) and (b), most of the functional groups peculiar to the component reagents were observed but in figs 4.3 (c) and (d), chemical reactions of the component reagents and the increase in the concentration of the functionalized TiO_2 nanoparticles from 2%-4% are responsible for the extinction of the functional groups as a result of oxidation and hydrolysis.

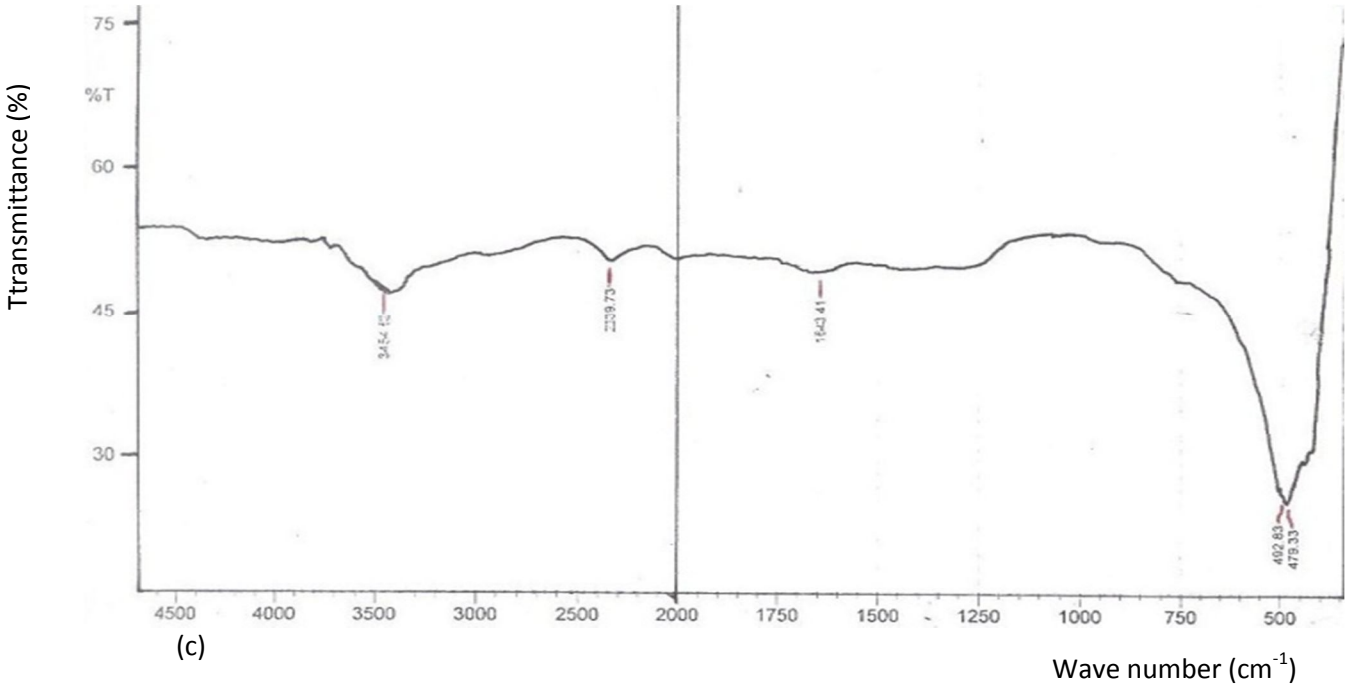
From fig 4.3 (a-d) and table 4.3, it can equally be deduced that the OH stretching vibrations of the intermolecular hydrogen bonding occurring in the range 3427.62cm^{-1}-3483.56cm^{-1} is basically due to the adsorbed H-O-H. Organics (methylene groups) were also represented by the ν_{as} CH_2 asymmetrical stretching vibrations in ranges slightly above 2910cm^{-1}. The CH stretching vibrations with coexisting terminal triple bonds resulting from remnant alkyne groups occur in the range 2067.76cm^{-1}-2145.88cm^{-1}. All the changes observed in the vibration frequency of νC=O in the blend indicates the incorporation of the nanofillers (TiO_2) has great influence on the vibrational frequency of νC=O. Furthermore, conjugation with CH_3 (phenyl groups) results in an increase in bond length of C=O thereby creating functional sites on the surface of the polymer blend. The C-O-C vibrations in esters occurring in the frequency ranges


Ttransmittance (%)
%T
80
60
40
20
4334.19
4173.13
4014.66
3483.56
2895.25
2813.63
2384.10
2240.39
2165.17
1987.48
1726.35
1645.33
1465.95
1358.00
1284.63
1139.97
1078.32
950.94
843.88
718.51
524.66
383.85
4500
4000
3500
3000
2500
2000
1750
1500
1250
1000
750
500
Wave number (cm-1)

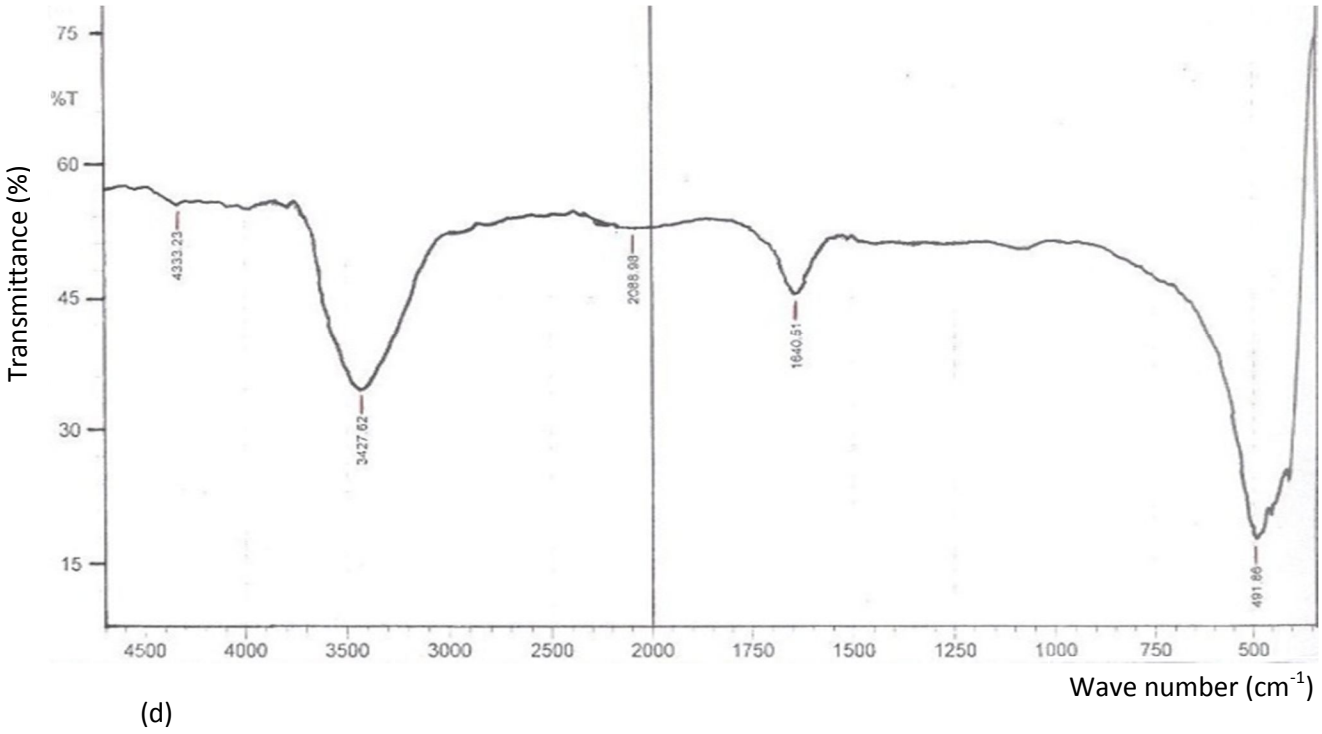
(a)


Transmittance (%)
%T
30
25
20
15
10
5
3482.59
2915.50
1647.26
1454.98
1384.27
1293.31
1104.28
949.01
841.96
699.88
4500
4000
3500
3000
2500
2000
1750
1500
1250
1000
750
500
Wave number (cm-1)

(b)



(c)



(d)

Fig 4.3: FTIR Spectra of Polymer blend/ TiO_2 Nanocomposites containing:

(a) 1% of TiO_2 (b) 2% of TiO_2 (c) 3% of TiO_2 and (d) 4% of TiO_2

949.01cm^{-1}-950.94cm^{-1} and 1284.63cm^{-1}-1293.31cm^{-1} represent the possible combination of acetate and alcohol groups. Finally, the functional groups appearing in the range 383.85cm^{-1}-491.66cm^{-1} represent Ti-O bonds of the functionalized TiO_2 nanoparticles.

Table 4.1: Assignment of Different IR Peaks of Polymer Blend/TiO_2 Nanocomposites with the Corresponding Absorption Bands

S/N	Band Assignment	Absorption Band (cm^{-1})				
		Functionalized TiO_2 using Stearic Acid	99% Blend with 1% F_N TiO_2	98% Blend with 2% F_N TiO_2	97% Blend with 3% F_N TiO_2	96% Blend with 4% F_N TiO_2
1	vOH (m) Intermolecular Hydrogen Bonding (stretching vibration)	3269.45-3590.61 (w)	3483.56	3482.59	3454.62	3427.62
2	=C-H (w) stretching vibration	3045.70	----	----	----	----
3	v_{as} CH_2 (s) asymmetrical stretching vibration (organics)	2930.93 (w)	----	2915.50	----	----
4	v_a CH_2 (s) symmetrical stretching vibration (organics)	2859.56	2613.13-2895.25	----	----	----
5	O=C=O (for CO_2) (w)	----	2384.10	----	2339.73	----

6	C-C≡C-C≡CH (w) stretching vibration	----	2165.17-2240.39	----	----	2088.98
7	vC=O (m) stretching vibration (carbonyl)	1634.73 (w)	1645.33-1967.46	1647.26	1643.41	1640.51
8	vCH_2-O (s), C-H in-plane bending vibration	1448.59 (w)	1465.95	1464.26	----	----
9	σ_{as} CH_3 (s) asymmetrical bending	----	1356.00	1354.07	----	----
10	C-O-C (s) stretching vibration in esters	----	950.94, 1284.63	949.01, 1293.31	----	----
11	C-OH (w) stretching vibration (acetate/alcohol group)	----	1076.30-1139.97	1104.28	----	----
12	Ti-O-Ti-C_nH_m (s) bending vibration	715.61-886.32	718.54-843.88	841.96	----	----
13	v_{as} Ti-OH (w) asymmetrical bending	640.39	----	----	----	----
14	v_{as} Ti-C (b) asymmetrical bending	598.92 (w)	----	599.88	----	----
15	v_s Ti-O-Ti (s) symmetrical bending	512.22	383.85-524.66	----	479.33-492.66	491.86

			(m)			

where, w = weak, s = strong, m = medium and b = broad.

4.3 X-ray Diffraction Analysis of Polymer Blend/TiO_2 Nanocomposites

The crystallinity of polymer blend /TiO_2 nanocomposites was characterized using X-ray diffractometer (Phillips X'pert X-Ray Diffractometer) employing a 1.54060Å copper X-ray source. The samples were scanned from 2θ = 5-80^o using a step size of 0.06^o. The percentage crystallinity (X_c) was calculated following the procedure as proposed by Eichhorn et. al. (2001) with the Scientific Graphing and Data Analysis Software (Origin 8.0), using the following equation:

$$X_c = \frac{A_c}{A_c + A_a} \qquad (4.1)$$

where X_c, (percentage crystallinity), is the ratio of crystalline peak area (A_c) to the sum of the crystalline peak area (A_c) and amorphous peak area (A_a).

The average crystallite size corresponding to structure order of the pattern was also calculated from integral breadth of the peaks according to Scherrer's equation (Patterson, 1939).

$$D_c = \frac{K\lambda}{ß \cos\theta}, \qquad (4.2)$$

where ß is the Full Width at Half Maximum (FWHM) of the peaks in radians, θ is the Bragg angle in degrees and K has a value of 0.9 and is called Scherrer's constant.

The value of the interplanar spacing between the atoms in the crystal, **d** was calculated using the Bragg equation;

$$n\lambda = 2d \sin\theta. \qquad (4.3)$$

where $n = 1$ is an integer, λ is the wavelength of the X-rays, d is the spacing of the planes of atoms and θ is the angle of incidence of x-ray beam. The d-spacing values are given in Table 4.2 (a-d) and the diffraction patterns presented in fig 4.4 (a-d) are plots of scattering intensity versus the scattering angle 2θ.

The uneven baseline in the XRD patterns for all the samples is due to the large amount of amorphous polymer content. The addition of TiO_2 nanoparticles to the polymer blends improved the crystallinity of the composites. The diffraction peaks in the range 2θ = 15-20^o can be linked to crystalline behaviour of the polymer blends. The peaks at 2θ = 19.66^o, 19.84^o, 20.34^o, and 20.49^o with d-spacings d = 4.5154Å, 4.4742Å, 4.3642Å and 4.3325Å indicate the presence of crystalline structure of PVA, consistent with the works of G'eminarda *et al.,* (2005) and Lee *et al.*, (2006).

Table 4.2: Peaks positions (2θ), d-spacing and Relative Intensity of Polymer Blend/TiO_2 Nanocomposites.

(a) 1% TiO_2

S/N	Peak Position, 2θ (^{o})	d-spacing (Å)	Relative Intensity (%)
1	16.84150	5.26447	30.8
2	18.58370	477469	100.0

3	20.49970	4.33254	41.8
4	22.99860	3.86714	62.64
5	35.62810	2.51999	6.2

(b) 2% TiO_2

S/N	Peak Position, 2θ (°)	d-spacing (Å)	Relative Intensity (%)
1	22.20220	4.00401	54.9
2	25.50810	3.49210	100.0
3	26.24360	3.39587	41.2
4	31.77600	2.81613	8.6
5	35.51800	2.52755	19.6

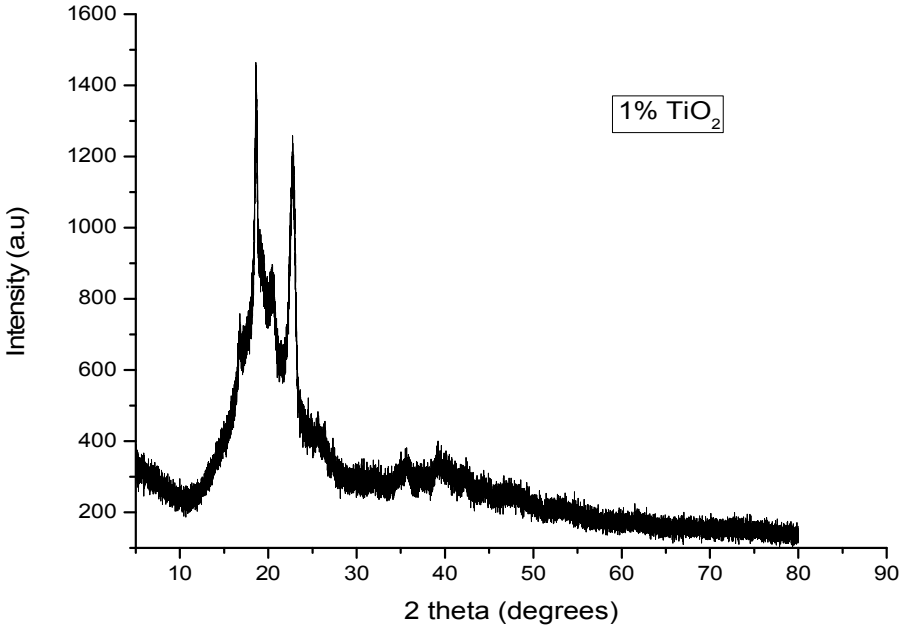
(c) 3% TiO_2

S/N	Peak Position, 2θ (°)	d-spacing (Å)	Relative Intensity (%)
1	16.18800	5.47549	15.8
2	17.99380	4.92986	77.5
3	19.84370	4.47427	25.9
4	22.12880	4.01713	100.0
5	25.02950	3.55776	8.7
6	34.94940	2.56735	5.3

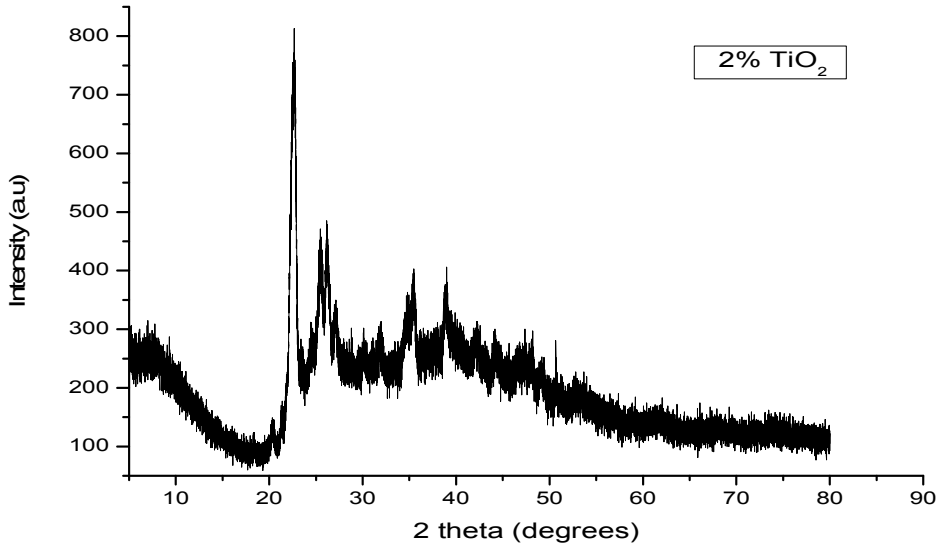
(d) 4% TiO_2

S/N	Peak Position, 2θ (°)	d-spacing (Å)	Relative Intensity (%)
1	17.84200	4.97148	65.6
2	19.66090	4.51544	42.9

3	21.91470	4.05589	100.0
4	23.89970	3.72334	49.5
5	46.72110	1.94428	19.4
6	52.65040	1.73700	9.74

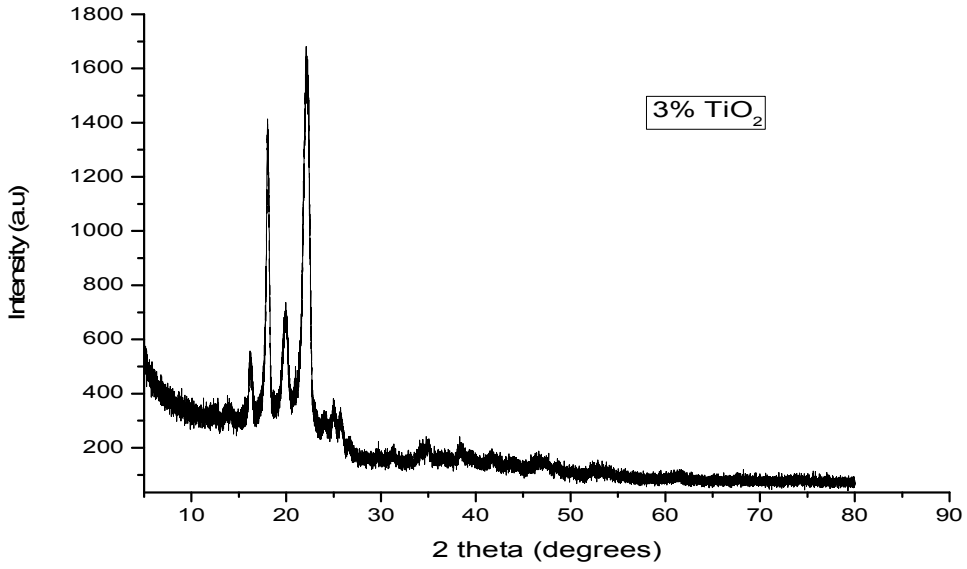


(a)

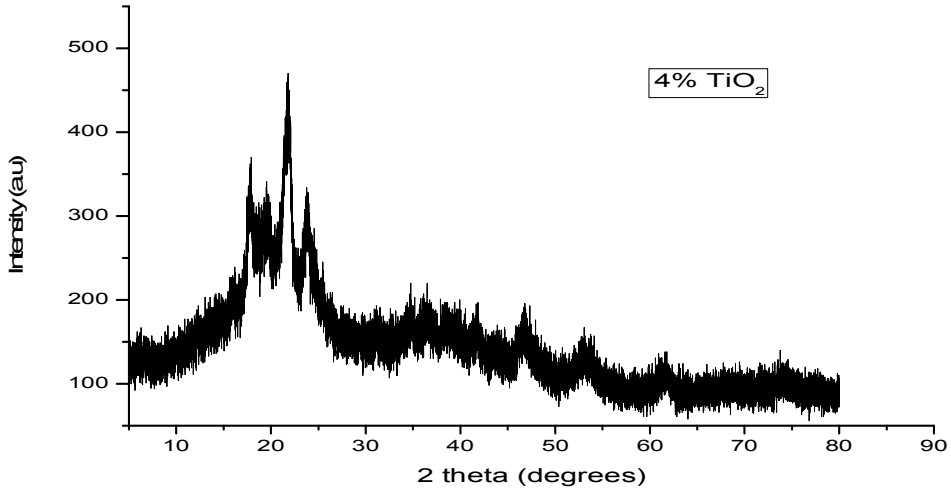


(b)

Fig 4.4: X-ray Diffraction Patterns of Polymer Blend/TiO_2 Nanocomposites containing (a) 1%, (b) 2% of TiO_2.



(c)



(d)

Fig 4.5: X-ray Diffraction Patterns of Polymer Blend/TiO_2 Nanocomposites containing (c) 3%, (d) 4% of TiO_2.

Furthermore, the XRD patterns of polymer blend/TiO_2 nanocomposites reveal the crystal structures of TiO_2 but few peaks representing TiO_2 phase have been shifted slightly to lower 2θ values (2θ = 21.9147°, 22.1288°, 22.3682°, 22.4479°, 22.77578°, 22.8024° and 22.9986°) due to slight expansion of TiO_2 structure as a result of surface modification and bonding with the polymer blend matrix. This is also consistent with the works of Shuqiang *et al.,* (2007) and Yang *et al.,* (2009).

The average crystallite size values, D_c of the polymer blend/TiO_2 nanocomposites are calculated and presented in Table 4.3 with values ranging from 1.69 ± 0.29 μm (1687.93 nm) to 4.59 ± 0.13 μm (4589.04 nm). The percentage crystallinity values of the polymer blend/TiO_2 nanocomposites are given in Table 4.3 with values ranging from 56.9 ± 0.2% to 67.6 ± 0.7%. The sample with 4% TiO_2 content displayed higher percentage crystallinity compared to other samples.

Table 4.3: Calculated Values of the Average Crystallite Size, D_c(nm) and Percentage Crystallinity, X_c(%)

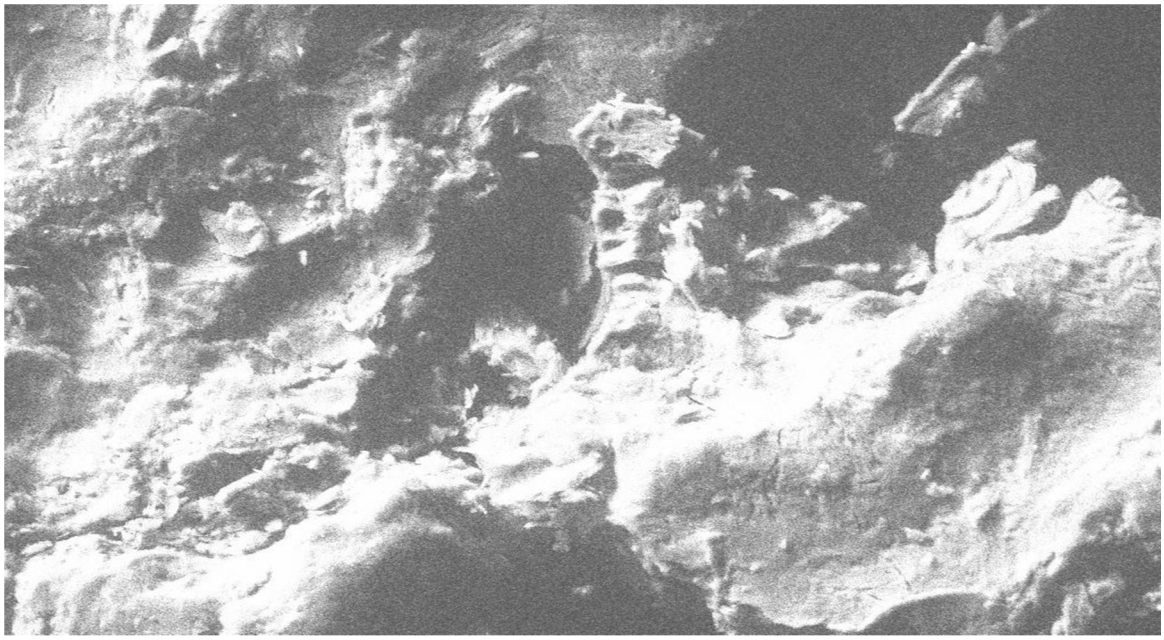
S/N	Sample	Average Crystallite Size, D_c(nm)	Percentage Crystallinity, X_c (%)
1	Polymer Blend Containing 1 wt % of TiO_2	4589 ± 130	65.2 ± 0.5
2	Polymer Blend Containing 2 wt % of TiO_2	3909 ± 750	56.9 ± 0.2
3	Polymer Blend Containing 3 wt % of TiO_2	3764 ± 630	64.8 ± 0.4
4	Polymer Blend Containing 4 wt % of TiO_2	1688 ± 290	67.6 ± 0.7

4.4 Scanning Electron Microscopy (SEM) of the Polymer Blend/TiO_2 Nanocomposites

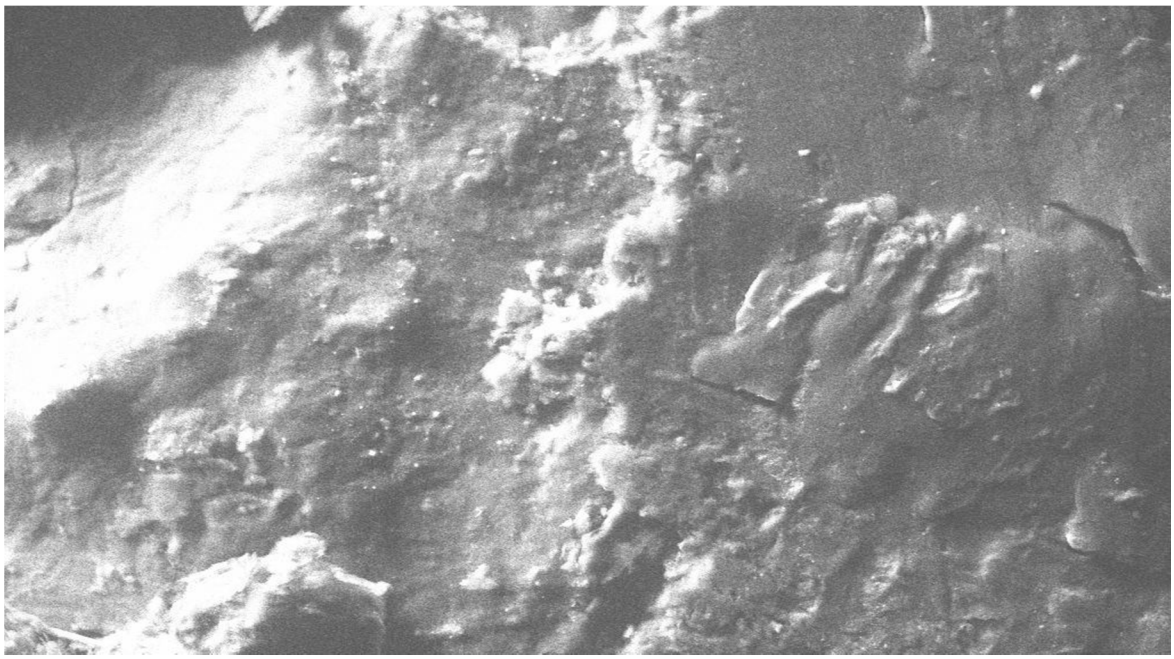
The surface morphology of the polymer blend/TiO_2 nanocomposites was observed using EVOIMA10 (ZEISS) multipurpose scanning electron microscope operating at 20kV employing secondary electron signals. The SEM images presented in Fig 4.5 (a-d) were observed at a magnification of 200X and the particle size distribution was obtained using imaging software (Image-J).

The microstructure of the polymer blend/TiO_2 nanocomposites reveal two distinct phases comprising of lighter modified TiO_2 nanoparticles and dark bulk polymer blend matrix. The lighter modified TiO_2 nanoparticles are evenly dispersed over the dark bulk polymer matrix with spherical shapes and the concentration increased with increasing content of the modified TiO_2 NPs (1%-4%) as depicted in Fig 4.5 (a -d).

The contrast observed in the SEM images (Fig 4.5) arises from atomic number difference, since phases within a material are dependent upon back scattered electron yield and the corresponding atomic number of atoms present within different phases. As such, the modified TiO_2 nanoparticles appear lighter compared to the bulk polymer blend matrix because the atoms present in TiO_2 phase have higher atomic numbers and higher back scattered electron yield.

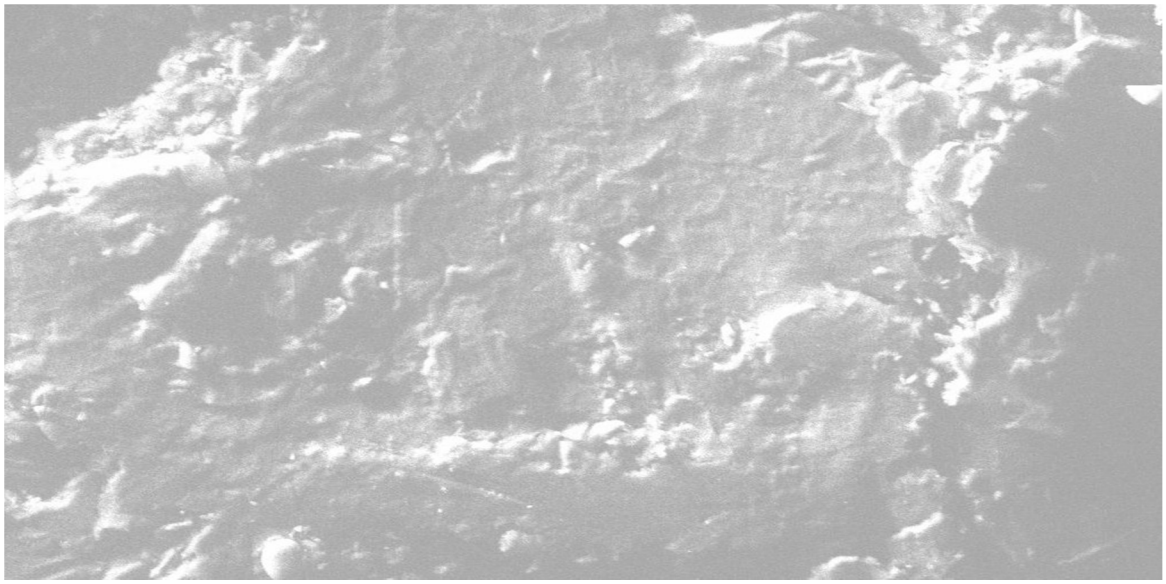


(a)

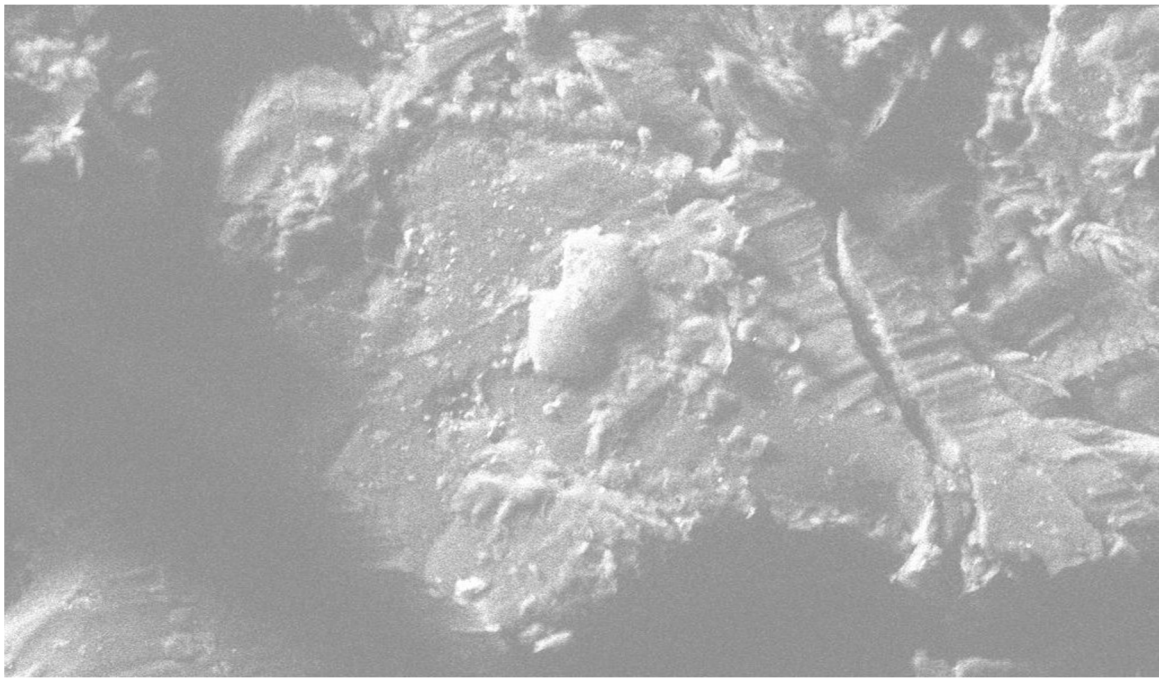


(b)

Fig 4.6: Scanning Electron Microscopy Images of Polymer Blend/TiO_2 Nanocomposites containing: (a) 1%, (b) 2% of TiO_2. [scale 1:20, magnification X200].



(c)



(d)

Fig 4.7: Scanning Electron Microscopy Images of Polymer Blend/TiO_2 Nanocomposites containing: (c) 3% and (d) 4% of TiO_2. [scale 1:20, magnification X200].

The average particle diameters of the polymer-blend/TiO_2 nanocomposites as determined from SEM images using imaging software (Image J) are presented in table 4.4 below.

Table 4.4: Average Particle Diameters of Polymer Blend/TiO_2 Nanocomposites from SEM Images.

s/n	Sample	Average Particle Diameter (µm)
1	Polymer Blend/1 wt % of TiO_2	119 ± 5
2	Polymer Blend/2 wt % of TiO_2	129 ± 5
3	Polymer Blend/3 wt % of TiO_2	174 ± 3
4	Polymer Blend/4 wt % of TiO_2	179 ± 4

4.5 UV-Visible Spectrophotometry

All the samples prepared were scanned in the ultraviolet (UV) radiation wavelength range of 200 nm-400 nm and visible radiation wavelength range of 400 nm-900 nm using JENWAY 6405 UV-Visible spectrophotometer at Ahmadu Bello University Multi-User Science Research Laboratory. This analysis is carried out to study the absorption/filtering property of the nanocomposites produced.

Changes occur when atoms or impurities are incorporated into a pure matrix (polymer, semiconductor, metal etc), because their environment is neither inert nor isotropic. This anisotropy may lead to resonant coupling between the photons (in this case, UV-Vis component of the electromagnetic spectrum) and the collective modes of (electronic transitions/excitations) of the polymer nanocomposites when exposed to UV-Visible light. The interaction of the UV-Visible light with the polymer nanocomposites may also give rise to polarization of the nanocomposite matrix, which in turn

may be seen as variation in the magnitude of absorption/transmission with respect to changes in wavelengths (i.e. 200-900 nm) when examined using UV-Vis spectrophotometer. In addition to this, anisotropy of the nanocomposite matrix resulting from addition of TiO_2 nanoparticles gave rise to varied properties as a result of slight structural modifications. These structural modifications have been studied using FTIR, XRD and SEM.

4.5.1 UV-Vis Spectra of Polymer blend/TiO_2 Nanocomposites

The UV-Vis spectra of for the polymer blend are presented and discussed below. The slight variation in the percentage absorbance over wavelength range (i.e. 200-900nm) is attributed to the TiO_2 nanoparticles content (1-4%) in each sample.

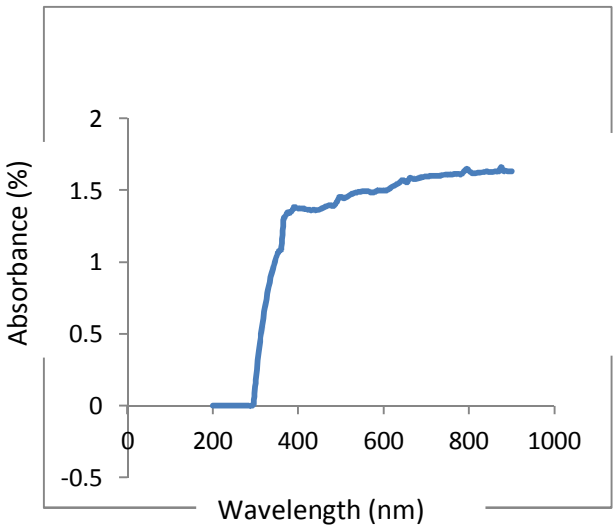
The UV-Vis spectra of polymer blend/TiO_2 nanocomposites are given in fig 4.8 (a-d).

The plot for blend sample (containing 1 wt % of nanoparticles) is presented in fig 4.8(a). The material filters at the onset of ultraviolet radiation wavelength through 295nm above which it absorbs significantly and rapidly until maximum absorbance of 1.385% is recorded at a wavelength of 390 nm. Slightly above the visible range, there is little decline in absorbance but appreciates reasonably through the whole range with maximum absorbance of 1.663% recorded at a wavelength of 795 nm.

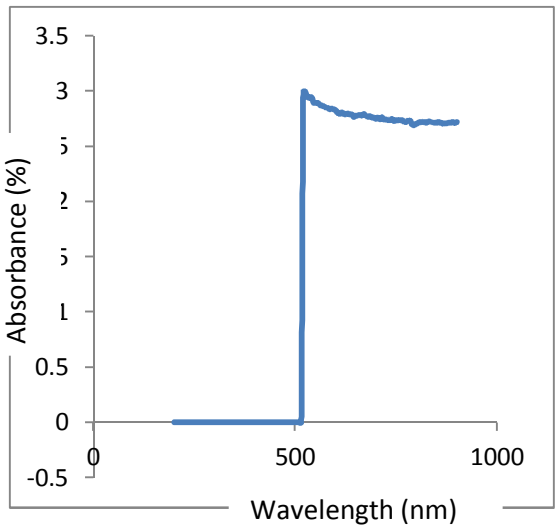
The material has displayed excellent property of being an ultraviolet radiation filter at low wavelengths (<300 nm) and absorber at higher wavelengths (300-400 nm) of the UV range in addition to being an excellent visible absorber.

Fig. 4.8(b) portrays the behaviour for blend sample containing 2 wt % of nanofillers. The spectrum shows absolute transparency from the onset of ultraviolet radiation wavelength range through a visible wavelength of 515 nm. A much significant absorbance of 2.997%, the maximum, is

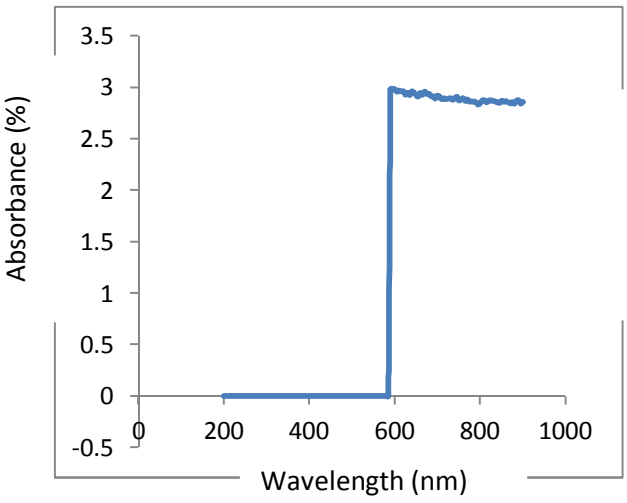
recorded slightly above that (i.e. at 520 nm) from which the absorbance decreases very slightly with a minimum of 2.708% at 800 nm. This material is an excellent UV filter and a very good visible radiation absorber.



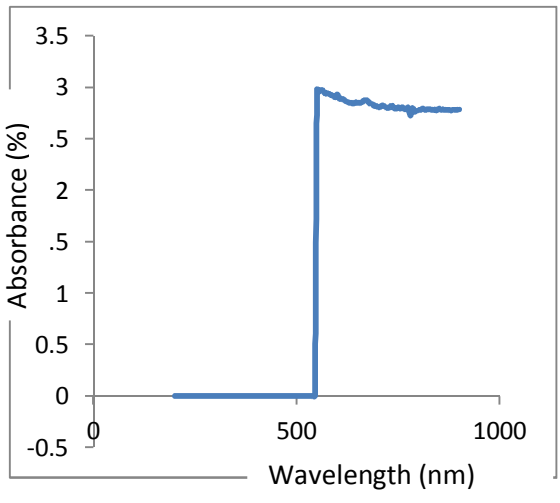
(a)



(b)



(c)



(d)

Figure 4.8: UV-Vis spectra of Polymer-Blend/TiO_2 Nanocomposites containing: (a) 1%, (b) 2%, (c) 3% and (d) 4% of TiO_2.

A similar behaviour to sample above is observed in both the remaining blend samples (with 3 wt % and 4 wt % of nanofillers respectively) as depicted in figures 4.8(c and d). However, there are slight shifts in the onsets of absorption, with the sample containing 3 wt % of TiO_2 having onset at a wavelength of 590nm corresponding to maximum absorbance of 2.983% and that containing 4 wt % of TiO_2 having onset at 550 nm corresponding to maximum absorbance of 2.982% as well. The minimum absorbance for these samples are recorded at 795 nm (2.835%) and at 780 nm (2.729%) respectively.

CHAPTER FIVE

SUMMARY, CONCLUSION AND RECOMMENDATIONS

5.1 SUMMARY

The elaborated synthetic technique has been developed to synthesize polymer blend (poly (vinyl alcohol) + poly (vinyl acetate))/TiO_2 nanocomposites which have the modified nanopowder covalently bonded onto the polymer chains. Several characterization techniques, such as EDS, FTIR, XRD, SEM and UV-Vis were employed to provide evidence for initial nanoparticle size, the success of appropriate chemical bonding, optical properties, and their particle diameter.

5.2 CONCLUSION

The synthesis of the nanocomposites was effected by surface modification. The objective of the first step was to turn the character of the surface into functional sites and to improve dispersion of nanoparticles in organic media.

FTIR spectroscopy was used to get evidence of how TiO_2 nanopowder existed in the polymer blend matrix. The analysis proved that the covalent chemical bonding between the polymer chains and inorganic phase was present in these hybrid nanocomposites.

X-ray diffraction analysis of the synthesized samples gives excellent percentage crystallinity values, (X_c) of 65.2 ± 0.5%, 56.9 ± 0.2%, 64.8 ± 0.4% and 67.6 ± 0.7% for the polymer-blend samples containing 1%, 2%, 3% and 4% of TiO_2 nanoparticles as well as average crystallite size values, D_c as 4589 ± 130 nm, 3909 ± 750 nm, 3764 ± 630 nm and 1688 ± 290 nm for the four samples respectively.

It was observed by SEM analysis that the dispersion of TiO_2 nanoparticles in the polymer matrix was relatively uniform. Also the particles had a very good adhesion with polymer domain, showing two

distinct phases of lighter modified TiO_2 nanoparticles and dark bulk polymer blend matrix. Average particle diameters were determined from SEM images using Imaging software (Image J) as 119 ± 5 µm, 129 ± 5 µm, 174 ± 3 µm and 179 ± 4 µm for 1%, 2%, 3% and 4% TiO_2 doped polymer blend samples.

Investigation with UV-Vis spectroscopy revealed that the dispersion of TiO_2 nanoparticles could improve optical properties of the polymer blends. The fact that nanocomposites displayed some level of transparency at lower wavelengths indicates that the nanoparticles are not agglomerated. In addition, strong UV absorption in some of the nanocomposite samples was observed because of the incorporated TiO_2 particles. In fact, with the exception of sample with 1% content of nanofiller, all the samples transmit UV radiation and absorb visible radiation at wavelengths of 520 nm, 590 nm and 550 nm for 2%, 3% and 4% doping. Thus the synthesized samples could act as an efficient optically transparent UV filter and visible radiation absorber.

5.3 RECOMMENDATIONS

This research work, as highlighted earlier, is limited to the synthesis and characterization of polymer blend/TiO_2 nanocomposites using FTIR, UV-Vis Spectrophotometry, XRD and SEM. It is, thus, recommended that further characterization be carried out using advanced techniques like Transmission Electron Microscopy (TEM) due to its sufficient contrast for the transmitted electrons between the polymer matrix and the nanofillers.

Thermal analysis should also be carried out in order to measure the physical and chemical properties of the nanocomposites as a function of temperature. This can be achieved using Thermogravimetric Analysis (TGA) which automatically records the change in weight of a sample as a function of either temperature or time and the Differential Thermal Analysis (DTA) which measures the difference in temperature (ΔT) between a sample and an inert reference material as a function of

temperature. Differential Scanning Calorimetry (DSC) should also be employed to determine the glass transition temperature (T_g) of the nanocomposites. This will help in controlling the extent of doping in the materials.

Electrical properties like conductivity, dielectric properties etc as well as mechanical properties including tensile and impact tests should be studied to verify the improvements due to the inclusion of the chosen TiO_2 nanoparticles.

This further characterization will widen the horizon of physical applications of the synthesized polymer blend/TiO_2 nanocomposites.

REFERENCES

Alexandre, M. and Dubois, P. (2000): Polymer-Layered Silicate Nanocomposites: Preparation, Properties and uses of a new Class of Materials. Mater. Sci. Eng., R., 28, 1-63,

Askeland D. R. (1985): The Science and Engineering of Materials, PWS publishers, 332-380.

Avadhani, C.V. and Chujo, Y. (1997): Polyimide-Silica Gel Hybrids Containing Metal salts: Preparation via the sol-gel Reaction. Appl. Organometal. Chem. 11, 153-161.

Berta, M., Lindsay, C., Pans, G. & Camino, G. (2006): Effect of Chemical Structure on Combustion and Thermal Behaviour of Polyurethane Elastomer Layered Silicate Nanocomposites, Polym. Degrad. Stabil., 91, 1179-1191.

Brass, M.L., Wilkie, C.A. & Bourbigot, S. (1998): Fire Retardancy of Polymers, RSC,.

Carrado, K.A. and Xu, L. 2005: In situ Synthesis of Polymer-clay Nanocomposites from Silicate gels. Chem. Mater., 10, 1440-1445.

Chandra, A., Turng, L.S., Gopalan, P., Rowell, R.M. & Gong, S. (2008): Study of Utilizing Thin Polymer Surface Coating on nanoparticles for Melt compounding Polycarbonate/Alumina Nanocomposites and their Optical Properties, Composite Science and Technology, 68, 768-776.

Chen, X. & Mao, S.S. (2007): Titanium Dioxide Nanomaterials: Synthesis, Properties, Modifications, and Applications. American Chemical society, Chem. Rev., 107, 2891-2959.

Du, H., Xu, G., Chin, W., Huang, L. and Ji, W. (2002): Synthesis, Characterization and Non-Linear Optical Properties of Hybridized CdS-Polystyrene Nanocomposites. Chem. Mater. 14, 4473-4479,

Elodie, N., Detrembleur, C., Jerome, C. & Alexandre, M. (2009): Patent Activity in Manufacturing Organoclays for Nanocomposites Applications, Recent Patents on Materials Science, 2, 43-49.

Evora, V.M.F. and Shukla, A. (2003): Fabrication, Characterization and Dynamic Behavior of Polyester-TiO_2 Nanocomposites. Mater. Sci. Eng. A. 361, 358-366,.

Feynman, R. P. (1960): Eng. Sci. 23, 22.

Fleming, M.S., Mandal, T.K. & Walt, D.R. (2001): Nanosphere-microsphere Assembly: Methods for Core-Shell Materials Preparation. Chem. Mater., 13, 6, 2210-2216 .

G'eminarda, J.C. and Bonraya, D.H. (2005): Thermal Conductivity Associated with a Bead-Bead Content Decorated by a Liquid Bridge; An Experimental Study Based on the Response of a Chain Subjected to Thermal Cycles. Gayvallet Eur, Phys 48: 509-517.

Garcia Curiel, Maria Monserrat de la Luz (2004) : Polymer-Inorganic Nanocomposites; Influence of Colloidal Silica, A PhD thesis submitted to the university of Twente, Netherlands.

JECFA (2006): Published in FAO JECFA Monographs, 3.

Jeon, I.Y. & Baek, J.B. (2010): Nanocomposites Derived from Polymers and Inorganic Nanoparticles, J. of Appl. Polym. Sci., 111, 3654-3674.

Jordan, J., Jacob, K.I., Tannenbaum, R., Sharaf, M.A. & Jasiuk, I. (2005): Experimental Trends in Polymer Nanocomposites; A Review, J. of Mat. Sci. & Eng., A, 393, 1-11

Katz, D.A. (1998): Polymers, a lecture presentation.

Kim, S. & Marand, E. (2008): High Permeability Nanocomposite Membranes Based on Mesoporous MCN-41 Nanoparticles in a Polysulfone Matrix, Microporous and Mesoporous materials, 114, 129-136.

Kothurkar, N.K. (2004): Solid State Transparent Cadmium Sulfide-Polymer Nanocomposite, a Ph.D. Thesis, University of Florida.

Lagashetty, A. & Venkataramen, I. (2005): Polymer Nanocomposites, John Wiley and sons.

Lee, G.W., Park, M., Lee, J.I., Yoon, H.G. (2002): Enhanced Thermal Conductivity of Polymer Composites Filled with Hybrid Filler Composites Part A: Applied Sciences and Manufacturing, 37: 727-734.

Lee, S.S., Lee C.S., Kim, M.H., Kwak, S.Y., Park, M., Lim, S. Choe, C.R. & Kim, J. (2001): Specific Interaction Governing the Melt Intercalation of Clay with Poly (styrene-co-acrylonitrile) Copolymers, J. of Polym. Sci.: part B: Polym. Physics, Vol. 39, 2430-2435.

Liang, Y. Omachinski, S., Longsdon, J., Cho, J.W. & Lan, T.A. (2002) : A Technical Paper on Nanotechnology, nanocorporation Inc.

Manias, E., Polizos, G., Nakajima, H., and Heidecker, M.J. (2007): Fundamentals of Polymer Nanocomposite Technology, John Wiley & Sons, Inc. 31-66.

Manias, E., Zhang, J. & Huh, J.Y. (2009): Polyethylene Nanocomposite Heat Sealants with a Versatile Peelable Character, Macromol. Rapid Commun., 30, 17-23..

Masoud, S.N., Dawood G. (2009): Polymeric Nanocomposites Materials, J. of Alloy compd., 442-447.

Mohan, S., Lauren N.C., Surya, S.G. & Karen, I.W. (1996): Melt Intercalation of Polystyrene in Layered Silicates, J. of Polym. Sci.: part B: Polym. Physics, Vol. 34, 1433-1449.

Morgan, A.B. & Wilkie, C.A. (2007): Flame Retardant Nanocomposites. Wiley Publishing/CRC Press.

Okamoto, M., Morita, S., Kim, Y.H., Kotaka, T. and Tateyama, H. (2000): Synthesis and Structure of Smectic Clay/Poly (methyl methacrylate) and Clay/Polystyrene Nanocomposites via in situ Intercalative Polymerization, Polymer, 41, 3887- 3890.

Onuma, M.K. (2010): A Study of the Physical and Electrical Behaviour of HDPE/$CaCO_3$ Nanocomposites, unpublished.

Pegoretti, A., Dorigato, A., and Penati, A. (2007): A Tensile Mechanical Response of Polyethylene-Clay Nanocomposites, express Polymer Letters, vol. 1, no.3, 123- 131.

Porter, D.B. (2000): Conference Proceedings from Organic-Inorganic hybrids conference Guildford, U.K.

Ratna, D. (2005): Epoxy Composites: Impact Resistance and Flame Retardancy, Rapra Review Reports, vol. 16, No 5.

Rosoff, M. (2002): Nano-Surface Chemistry, Marcel Dekker Inc., New York.

Russ, J. C. (1984): Fundamentals of Energy Dispersive X-ray Analysis, Butterworths, London.

Salavati-Niasari, M., Ghanbari, D. & Davar, F. (2009): Synthesis of Different Morphologies of Bismuth Sulfide Nanostructures via Hydrothermal Process in the Presence of Thioglycolic Acid. Alloy. Compd. 488: 442-447.

Sanchez, C., Juliana, B. Belleville, P. & Popall, M. (2005): Applications of Hybrid Organic-Inorganic Nanocomposites, J. of Mat. Chem., 15, 3559-3592.

Saujanya, C. & Radhakrishna, S. (2001): Polymer Nanocomposites, J. of Polym. Sci., 42, 6723-6731.

Saxena, S.K. (2004): Polyvinyl Alcohol, Chemical and Technical Assessment (CTA), FAO.

Shuqiang Jiao and Hongmin Zhu, (2007): Electrolysis of Ti2CO Solid Solution Prepared by TiC & TiO2, Journal of Alloys & Compounds, 438; 243-246.

Solomon, D.H. & Hawthorne, D.G. (1998): Chemistry of Pigments and Fillers, John Wiley and sons Inc., New York.

Suryanarayana, C. & Froes, F.H. (1992): The Structure and Mechanical Properties of Metallic Nanocrystals, Metall. Trans., 23, 1071-1081.

Taniguchi, J. & Ohkita, K. (1977): Testing Paper for Measuring Polyvinyl Alcohol Concentration. Japanese Patent to Shikishima Spinning Co., Ltd.

Tolstov, A.L., Matyushov, V.F. & Klymchok, D.O. (2008): Synthesis and Characterization of Hybrid Cured Poly (ether-urethane) Acrylate/Titania Microcomposites Formed from Tetraalkoxytitanate Precursors, Express Polymer Letters, 2,No 6, 449-459.

Vaia, R. & Wagner, D. (2004): Nanocomposites: Issues at the Interface, Materials Today.

Vaia, R.A. and Giannelis, E.P. (1997): Lattice Model of Polymer Melt Intercalation in Organically-Modified Layered Silicate, Macromolecules, 30, 7990-7999.

William, G.E., Aldo, B.A. & Jinweng, Z. (2005): Polymer Nanocomposites: Synthetic and Natural Fillers; A review. J. of App. Polym sci.

Williams, L. & Adams, W. (2007): Nanotechnology Demystified, McGraw-Hill companies, U.S.A.

Yang, Z., Choi, D., Kerisit, S., Rosso, K.M., Wang, D., Zhang, Z., Graffi, G. and Liu, J., (2009): Journal of Power Sources, 192, 588-598.

Yeum, J.H., Park, J.H., Kim, I.K. & Cheong, I.W. (2010): Electrospinning fabrication and Characterization of Water Soluble Polymer/Montmorillonite/Silver nanocomposite Nanofibers out of Aqueous Solution, comp. sci. and tech., 63, 2223-2253.

Yoshida, O. & Okamoto, M. (2006): Direct Melt Intercalation of Polylactide Chains into Nano-Galleries; Interlayer Expansion and Nanocomposite Structure, Macromol. Rapid Commun., 27, 751-757.